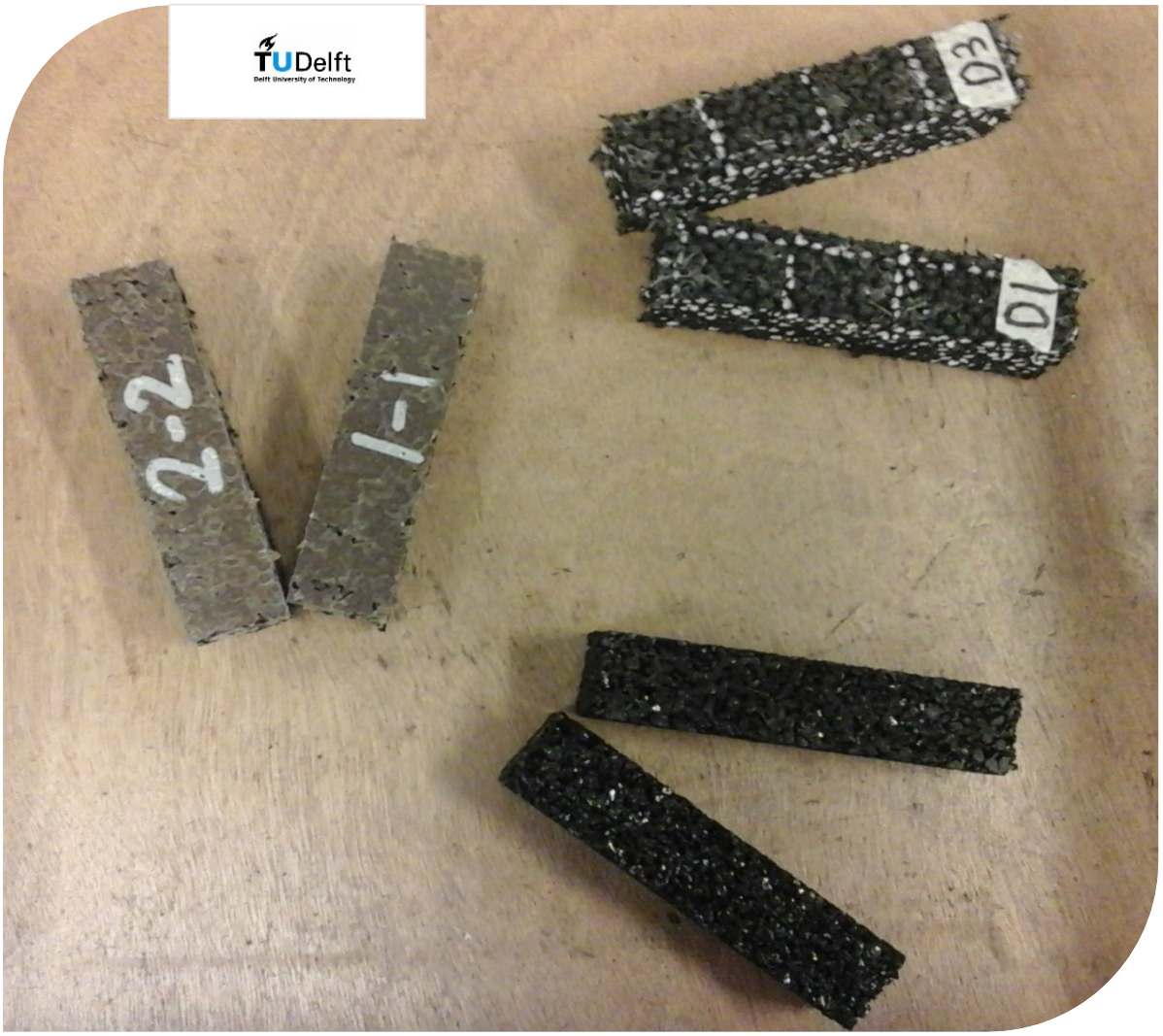

Determination of mechanical properties and water susceptibility of low-noise road surfaces

Georgios Pipintakos
Additional Master Thesis
4635248

Additional Master Thesis

by

Georgios Pipintakos

Student number: 4635248
Project duration: May 2017 – September 2017

Additional master thesis committee:
Prof. dr. ir. M.J.G. Sandra Erkens, TU Delft
Dr. Aikaterini Varveri, TU Delft, supervisor
Ir. Peter The, Rijkwaterstaat

Civil Engineering TU Delft
Department Pavement Engineering

This thesis is confidential and cannot be made public until 1/1/2020

Abstract

Nowadays, there is a need to reduce noise pollution due to the tyre-pavement interaction, especially in densely-populated areas, such as the Netherlands, where noise pollution is a major concern. A solution to this problem is the development of pavement surfaces with improved noise reduction characteristics. Previous attempts to develop low-noise pavement surfaces were not successful, mainly due to their poor mechanical performance and low durability. In this research the mechanical performance of three different low-noise pavement surface materials is investigated. The study was part of the Ultrastil Wegdek (USW) project in the Netherlands. The materials were evaluated with respect to their moisture susceptibility, stiffness, cohesive strength and bonding with the underlying layer. For three different low-noise road surfaces (LNRS), the stiffness was evaluated by means of dynamic modulus tests. Furthermore, indirect and direct tensile tests were carried out after long- and short-term moisture conditioning to estimate strength degradation. The interlayer bond strength was determined using uniaxial tension tests at dry and wet conditions. To evaluate the bond characteristics, also two-layer porous asphalt systems were tested as reference materials. The results show high difference in their properties as a result of the mixture composition. Especially, considering the effect of moisture is of paramount importance for these highly open-graded mixtures.

Preface

This research was part of the acquisition of my Master degree in Civil Engineering at the Technical University of Delft. It was performed by means of additional graduation work, independently from my Master thesis.

During this research, which was part of the USW project in the Netherlands, I performed all laboratory experiments in the pavement laboratory of TU Delft with the precious and truly appreciated help of Marco Poot and Michele van Angelen. However, I would have never been able to join this project, from which I gained experience and knowledge, without my daily supervisor Dr. Katerina Varveri. I would like to thank her for offering me this opportunity. I really enjoyed the discussions and explanations when I was confused with the results analysis.

Moreover, many thanks go to the head of my graduation committee Prof. Dr. Sandra Erkens for being there all the time, and providing me with valuable comments on technical capabilities of writing a technical report that will be also useful during my Master thesis. My final thanks go to Peter The who represented Rijkswaterstaat, for being a member of my assessment committee.

Georgios Pipintakos
Delft, January 2018

Contents

1. Introduction

1.1. Thesis framework

This thesis was part of the second phase of the Ultrastil Wegdek (USW) project, in which four (4) parties were involved: InfraQuest (Rijkswaterstaat, TNO and Technical University of Delft) and three market parties, namely Dura Vermeer, Intron and Heijmans. This additional thesis reports the results of the laboratory tests performed to characterize the mechanical performance of the low-noise materials developed in the USW project.

1.2. Ultrastil Wegdek (USW) project

1.2.1. Initiation

In the future years, a substantial increase in the traffic load is expected in the Netherlands. The increasing traffic together with an increase of the maximum allowable speed in the highways can lead to an increase of the noise pollution due to the tyre-pavement interaction. Traffic noise is often very annoying for people who live close to highways, and it is one of the main environmental factors that can have serious effects on health. It can lead to sleep disturbance, stress-related effects and even cardiovascular diseases. Especially, in densely-populated areas, such as the Netherlands noise pollution is a major concern.

In the beginning of 2014, the Ultrastil Wegdek (USW) project was launched. In this project, Rijkswaterstaat challenges the market to develop a low-noise road surface (LNRS) with a noise reduction of 10 dB(A) and a service life of at least seven (7) years.

In total, three market parties participate in the project: the Dutch construction companies Heijmans and Dura Vermeer and the Swiss-Dutch SGS Intron. The market parties develop their products with the financial support of Rijkswaterstaat (RWS). In this way, RWS offer the market the opportunity to develop innovative pavement materials. Delft University of Technology (TU Delft) and TNO also participate to the project and their main role is to advise RWS and perform all the required computational and experimental research to validate the new LNRS materials.

The project is organized in five (5) phases: preparatory, screening, main, semi-field and field-test. In the preparatory phase a project plan description was made for the main part of the project, which has been reported in report InfraQuest-2013-66 'IQ-PERS Experimental Work Plan'. Moreover, preliminary FEM analysis was planned for this phase. The proposed computational scheme and the results from the FE analysis were presented in the InfraQuest-2014-48 report 'Draft report on screening phase task 2.2.'. Furthermore, emphasis was placed on the interaction with the industry to individually assist them to optimize their currently available products. For this reason, a number of preliminary mechanical tests were performed based on the needs of each producer. Due to the fact that USW materials were still under development, the results of the mechanical tests were reported directly to the individual parties.

In the screening phase of the product, the products provided by the producers were tested for their noise reduction and wear characteristics by means of acoustics measurements and SR-IDT test, respectively. The products that qualified these tests were then able to proceed to the main phase of the project.

In the main phase of the project, the USW products and the individual mix components were tested for their mechanical performance. The mechanical tests were selected based on previous international experience with poroelastic surfaces and meant to address issues related to the durability and interlayer bonding of the USW materials. As a result the tests included moisture susceptibility, stiffness, interlayer bonding and cohesive strength tests. The ageing of the material over time was also taken into account by performing the same tests after ageing conditioning. According to the planning of the project, the developed USW materials were tested for their durability and interlayer bond strength in 2015. However, the results were not satisfactory. In November 2015, the advisory board advised the three market parties on how to further improve their mixture design. The most important issue for all USW products seemed to be the adhesion of the USW layer to the underlying ZOAB layer. In the view of the test results, the market parties were given additional time to improve their mixture design. The new USW products were tested for the same properties as earlier and the results of this phase are presented in this additional thesis.

In the semi-field test phase, the USW products will be tested in the STUVA APT facility in Germany. The USW products that will successfully pass the semi-field phase will be considered for field test sections.

1.2.2. Objectives

The main objective of the USW project is to develop a low-noise surface (LNRS) which leads to a noise reduction of 10 dB(A) and a service life of at least seven (7) years. Specific questions that would be addressed during the project are:

- Can the well-promising acoustic properties be combined with a long-term pavement service life?
- Do the new LNRS materials meet the technical requirements as set by the Dutch specifications for paving materials?

2. Present research work

2.1. Problem description

This thesis aims to give specific answers with respect to the mechanical behavior of the developed LNRS materials. The composition of the LNRS materials differs considerably from that of traditional asphalt mixtures. Even though these special mix designs impact the desired acoustic properties to the LNRS, it is also important that the LNRS fulfil several requirements regarding their durability and mechanical performance. Therefore, the main goal is to determine the mechanical properties of the materials at dry conditions, but also in the presence of water. Moreover, considering that the new materials will be used as a top surface layer, an investigation of their ability to bond properly with the underlying layer is of paramount importance. Hence, interlayer bond strength tests will be also performed.

2.2 Research objectives

The goal of this mini-research is to evaluate the mechanical performance of three different LNRS materials produced by the market parties as part of USW project. The main research questions that should be answered during this thesis are summarized below.

- What is the stiffness of the LNRS materials over a range of frequencies?
- How moisture affects the strength of each material?
- How good is the bond between the LNRS materials and the underlying ZOAB layer and how does bond strength degrade in the presence of water?
- How is the performance of the LNRS material compared to the reference two-layer ZOAB performance?
- What is performance-based the ranking of the newly produced LNRS materials?

2.3. Methodology

In this research study, a series of experimental tests were performed to evaluate the mechanical performance of the LNRS materials. Previous attempts for the development of low-noise materials failed in field sections due to various types of damages such as moisture damage, interlayer adhesion and skid resistance. The mechanical tests were selected, based on previous international experience with low-noise surfaces. In total three different tests were performed, namely dynamic stiffness modulus tests, moisture sensitivity tests and tensile bond strength tests. The results were post-processed, analyzed and are presented in Chapter five. Finally, the mentioned research questions were addressed and a first evaluation of the three LNRS materials was made.

2.4. Testing Plan

All tests were performed in a period of four (4) months. The duration of the tests was longer as long-term bath conditioning was required for some of the tests. The conditioning time for the moisture sensitivity tests was two (2) and four (4) weeks, while for the interlayer strength tests conditioning intervals of two (2), four (4) and six (6) weeks were specified. The planning of the tests was also based on the fact that the number of pulling stubs used for some tests was limited and their reuse was required. The main plan of the tests is presented in Table 1.

Table 1. Testing plan

Test	Conditioning					Execution				
	May	June	July	August	September	May	June	July	August	September
Stiffness Test										
Indirect tension Test										
Direct tension Test										
Tensile adhesive Test										

2.5. Thesis outline

All three (3) materials were tested for their stiffness, mixture strength and bond strength at different moisture conditions. A literature research for the development of low-noise materials is presented in Chapter three. In the fourth Chapter the experimental testing procedure, which was carried out for the three (3) materials is described in detail. In Chapter five the analysis of the test results as well as a short discussion of each outcome are presented. Finally, in Chapter six the main conclusions of this study are given.

3. Literature review

3.1. Low-noise pavements

3.1.1. Introduction

Nowadays, pavement engineering has developed materials in order to succeed the reduction of traffic noise mainly produced by the tyre-road system, as car manufacturers have almost entirely eliminated the engine noise at low speeds. Two main parameters can improve this phenomenon, namely higher quality tyres and the pavement structure. The pavement parameters that basically contribute to the reduction of noise are the pavement texture, the absorption of noise by the pavement and the elasticity of the pavement [1]. Low noise pavements with high void content and consequently with high absorption percentage and optimized texture are widely used in the Netherlands. The idea of making the pavement more elastic developed initially the investigation of poroelastic road surfaces (PERS) which stand for poroelastic road surfaces. According to terminology, PERS is defined as:

'A wearing course for roads with a very high content of interconnecting voids so as to facilitate the passage of air and water through it, while at the same time the surface is elastic due to the use of rubber (or other elastic products) as a main aggregate. The design air void content is at least 20 % by volume and the design rubber content is at least 20 % by weight' [2] .

3.1.2. Projects on low-noise pavements

Several efforts had been made to reduce noise from carriages and horses before asphalt pavement was widely used. Straw was put on cobblestone or stone sett pavements and thanks to its porosity and elasticity was able to reduce noise. This method was used outside hospitals and outside homes of rich people [3].

PERS was initially invented in the late 1970s by Nils-Ake Nilsson in Sweden as part of a project that he was working on with his acoustic consultancy company IFM Akustikbyran AB in Stockholm. By that time only some acoustic laboratory experiments had been made indicating a reduction in tyre-road of 5 dB(A) compared to regular dense asphalt concrete (DAC). The porosity of the PERS materials used ranged from 35 to 40% and the materials were either elongated fiber-like rubber particles or granules of rubber glued with polyurethane. The rubber was obtained from scrap tyres [3]. During the 1980s some initial trials in Sweden increased the noise reduction to 10 dB(A). Only very simplified tests of wear, rolling resistance and durability were performed at that time. These trials were performed at a closed-down airport without traffic for 10 years, at a Stockholm street to check durability and at a two-lane local street. The second trial failed during winter while testing whereas the road surface in the local street had to be removed because of the loosening of the patches from the base course [3].

In 1989, a large project began in Oslo. A 130 m track with a surface, which included rubber granules glued with 13% polyurethane, was laid on a porous base [3]. The void content was 35% and its thickness was 19mm. The new surface led to a reduction of the measured noise up to 7-9 dB(A) compared to DAC, but showed an unacceptable friction coefficient of 0.36, when measured with 'Mu-meter' [3]. After the laying of the surface, small patches loosened in one of the two lanes of the track. However, in the beginning of winter large parts were detached under snow conditions and finally the road was removed.

In 1996 Acoustic Control AB in Stockholm developed a poroelastic road surface with large percentage of rubber granulates mixed with sand glued with bituminous binders [3]. The variations of rubber and sand percentages were investigated as well as the type of rubber granulates. Although it led to a noise reduction of 12-14 dB(A) compared to conventional dense asphalt, the details of the composition and tests performed remained unknown to the public [3].

The next century Public Works Research Institute (PWRI) in Japan tried and succeeded to obtain a reasonable service life using a variety of LNRS types. After some initial laboratory testing, outdoors tests were performed in 1996 on a test track by allowing the repetitive passage of heavy trucks as an indication of durability; the test track resisted about 180000 truck passes [3]. The base course was DAC and soon delamination occurred at the interface between the layers at specific spots of the test section. The mix design included elongated fiber-like rubber particles glued with 15% of polyurethane. Fire safety tests for rubber were also performed on different types of pavements namely porous asphalt (PA), dense and poroelastic mixtures sprinkled with gasoline. Poroelastic found to be safer than DAC but not than PA. Simultaneously, a test track was paved in Japan in 1996 with high percentages of air voids i.e. 30, 35 and 40% and led to reduction of noise of 7-11 dB(A) for cars, 4-5 dB(A) for light truck and 3-5dB(A) for heavy truck compared to DAC [3].

Because of the low friction coefficients observed initially in PERS, four different types of PERS materials were developed and tested for wet friction with a vehicle that measured dynamic friction. The tests showed that an improved behavior can be achieved thanks to the addition of texturing materials such as small sand grains [3].This new generation of PERS was also glued with epoxy and not polyurethane and led to better adhesion with the base course. In other Japanese cities such as Mie, Akita, Zama and Yokohama a lot of test tracks were built-up with significant noise reduction up to 10 dB(A) comparing with DAC between 2002 and 2006. The main failures that appeared were rutting, adhesion with the base course and too low wet friction coefficients. Many efforts to address these problems were made such as grinding of the base course to make it smoother and improve the adhesion [3].

A PERS test section of 20 m was laid on a highway in Akita and opened to traffic in 2002. This surface was a 30 mm layer glued with epoxy on a base block of cement concrete. It included hard plastic pieces to increase friction and recycled fiber-like rubber from truck tyres glued with polyurethane as binder. Finally it failed because of rutting, not due to the compression or the wear of rubber, but due to displacement of the intermediate layer of asphalt-coated sand on which the surface was placed [3].

In addition, in Zama city a different type of PERS by Yokohama Rubber Company was used. It included rubber and stone/sand aggregates in order to improve the skid resistance, air voids content was 30% and a polyurethane binder that was cured for 1 hour [3]. Carbon black was added to give a darker surface. The problems that appeared were related to raveling along the joints between screeds. Also, the rolling resistance proved to be lower than DAC. However the new surface provided a noise reduction of about 10 dB(A) compared to DAC [3].

Among 2002 and 2008 several tests were carried out in the Netherlands to eliminate noise from road and rail under the Dutch Noise Innovation Programme (IPG) [3]. A part of this programme was the optimization of acoustic performance of road surfaces with construction of different road surface types with varying elasticity, porosity and texture. Initially in Kloosterzande, a town in the Dutch province of Zeeland, a non-trafficked road was measured for absorption, texture and elasticity. The results were used for a rolling noise prediction model, which is considered the most advanced acoustic optimization tool (AOT) so far [3]. The interest for PERS in the Netherlands continued afterwards with a project that started in 2008 and finished in 2011. The durability, safety and temperature effects were studied. A 40 m long test section was constructed in 2009 again in Kloosterzande using the Rollpave construction technique. The rolled-off PERS was 32 mm thick and included mixture of rubber and stone granules bound with polyurethane. An epoxy resin glue was used to glue the porous asphalt onto the base course and the obtained noise reduction was 7.9 dB(A) compared to DAC. Afterwards the mixture was modified and laid on a larger test section on A50 in Apeldoorn [3].

Figure 1. Construction of PERS road in Kloosterzande using Rollpave technique

In 2008 twelve partners from eight European countries developed the idea to make a proposal with the help of six road research institutes, two contractors, two specialist partners and two universities. The proposal was approved by the European Commission and the project poroelastic road surface for avoiding damage to the environment (PERSUADE) started in 2009 and finished in 2016. The main goal of this project was to combine the low-noise properties of these materials with a sufficient skid resistance properties and sufficient service life [4]. The main phases that distinguished in this project were laboratory, construction and monitoring phase. In laboratory phase, different mixtures designed and tested for sufficient requirements of skid resistance, interlayer bonding and noise reduction. An optimization of the mixture was investigated, with over 25 different mixtures designed, and reported as main problem the combination of sufficient skid with raveling resistance. During the construction, seven test tracks in five different countries were tested and the monitoring of them with a cost-benefit analysis was followed up [5].

The main conclusions were that a noise reduction of 8 to 12 dB(A) was obtained compared to dense mix asphalt 0/16, but also that construction failures may be proved unforgivable for the application of PERS layer. Such mistakes may be working in humid environment, which failed to protect the roller efficiently from particles sticking to it or letting the used tack layer cure too long before the application of PERS surface. Other common distress types such as raveling and loosening of patches were also reported in the full-scale tracks of PERSUADE [6].

3.1.3. Mix Design

There are different types of PERS including rubber granulates and mineral aggregates glued by an elastic resin, such as polyurethane [1]. The different percentages of these rubber and mineral aggregates are responsible for the resulting elasticity of the surface. These types of pavement lack completely or partly from bitumen. It has been shown that PERS materials with low bitumen contents can result in noise reduction of approximately 2 dB(A) compared to dense asphalt concrete (DAC), whereas the materials with total absence of bitumen lead to reduction of acoustic noise up to 12dB(A) compared again to DAC [4].

The different types of LNRS include rubber granules or fibers, usually blended with sand and stones or other additives. The origin of the rubber can vary and it may be either new or reused one. The binder used to bond the different particles is mainly polyurethane in ranging percentages from 5 to 17%. Moreover, a glue to fix the surface on the existing road base-course is required, and for this epoxy resins and bituminous binders are mainly used. The design of the material is based on a high volume of air voids, which ideally range from 25 to 40 % [2], in order to achieve the optimal behavior of the LNRS with respect to noise reduction and durability, but also keep up with the standard requirements of skid resistance. Finally, lower percentages of rubber aggregates ensure the flexibility of the material, but they lack of the required elasticity and for that reason are not included in LNRS [2].

3.1.4. Noise Generation

There are mainly three main mechanisms that contribute to tyre-road noise, namely vibrational, aerodynamic and amplification mechanism [7].

The texture and tyre-tread impact generate the radial vibrations, which belong to the first mechanism of noise phenomena as presented in Figure 2 [7]. Among the parameters that highly reduce noise production is the size of aggregates, which are preferably small, similar to what is used in the top layer of the two-layer porous asphalt in the Netherlands. This results in low texture impact excitation to the tyre thread and simultaneously to low vibrations and noise emission. Nevertheless, tyre tread impacts cannot be avoided which means that tyre vibrations cannot be completely suppressed [7].

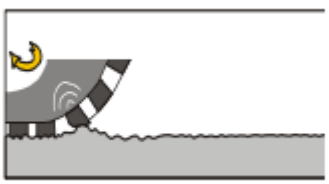

Figure 2. Radial tyre vibrations on road surface irregularities [5]

For the second category air pumping is the governing mechanism. The term air pumping is used to describe the phenomenon of a tyre running in a smooth surface, while the air is compressed at the leading edge of the tyre-road contact zone and is sucked-in at the rear edge (Figure 3). The high porosity of LNRS expressed via air void content allows the air to escape horizontally or vertically through the surface and leads to high reduction of the tyre pressure [7].

Figure 3. Air pumping, compression and suction of air [5]

For the third category, the horn effect is the governing mechanism. It is an amplification effect caused by the multiple reflections of noise in the contact zone between the tyre tread and a reflective road surface [7]. A high porosity surface reduces the horn amplification effect, as well as it works as sound absorber [2].

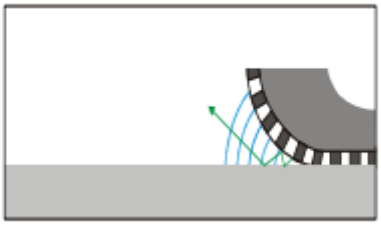

Figure 4. Horn effect [7]

Remarkable remains also the response of LNRS regarding the tyre-road impact mechanism. A significant difference of LNRS materials with hard surfaces is based on the fact that deflection of the tyre is taken as deflection of the LNRS, due to the flexibility of LNRS [7]. Consequently the angle of attack in the tyre-road surface is smaller, thus the impact is softer. Another aspect results from the lower and gradual deformation of tyre is that less vibration excitation occurs while rolling compared to hard road surfaces [2]. Moreover, the high porosity and air void content eliminates air pumping and horn effects. The elasticity of the surface as well as the smooth porous surface of an appropriately produced LNRS contribute to the exceptional acoustic properties compared to a hard surface. The findings of an experiment at two different road surfaces (elastic and concrete surface) presented in Graph 1 supports the previous argument [7].

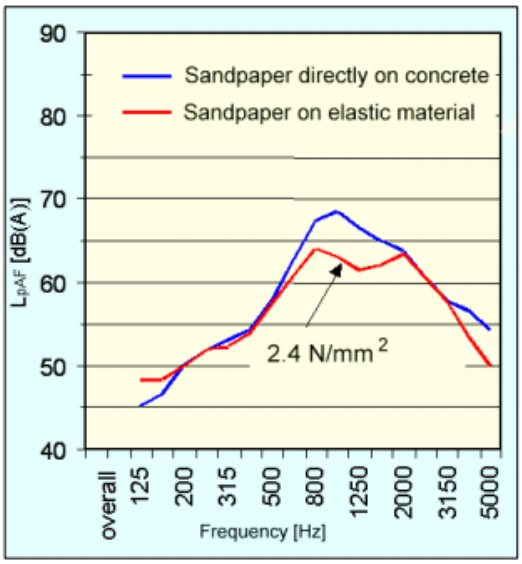

Graph 1. The effect of elasticity on tyre-road noise spectra [7]

3.2. Conclusions

The main failures reported in previous efforts of real field tests were the poor adhesion of the LNRS layer with the base course, low skid resistance, durability aspects and raveling in the presence of water. Based on the previous experience, the laboratory tests presented in this work were planned. The tests were performed at dry conditions, but aslo the effect of moisture on strength degradation was investigated.

4. Laboratory tests

4.1. Introduction

Based on previous projects with LNRS the main distress types related to durability, moisture damage and poor bond strength with the base course. For that reason, dynamic stiffness tests as well as cohesive strength and interlayer bond strength tests at various moisture conditioning intervals were performed. From now onwards due to confidentiality, we will refer to each material as Material A, Material B and Material C.

The three LNRS under study fulfill the air void content range of 25-40% according to the mix design and definition mentioned in the above. All three materials do not use bitumen as binder. Material A included rubber granulates in percentage 15-30% and aggregates (30-40%) glued with polyurethane (20-30%). The air void content ranged between 30 and 40%. Material B contains rubber (10-20%), aggregates (20-30%) polyurethane glue (40-50%) and results to an air-void content of 20-30%. Finally, the mixture of Material C lacks of rubber particles and contains aggregates (5-10%) again glued with a high percentage of polyurethane (55-65%). The air-void content is between 30 and 40%. Further information of the precise mix design is not included in this report, as this information is proprietary.

4.2. Dynamic Stiffness Test

4.2.1. Introduction

For bituminous mixtures it is crucial to estimate the performance of stiffness in a range of frequencies in order to use this information for the design of the pavement. In other words, it is important to know beforehand the performance of each course under traffic load as design criteria. It is directly connected with durability, fatigue life and crack initiation of the pavement.

For bituminous mixtures, two main categories of stiffness tests can be distinguished, homogeneous and non-homogeneous tests [8]. Homogeneous tests are directly related to stresses and strains and consequently to the constitutive law, whereas non-homogeneous take into account the geometry of the specimen to obtain the parameters of the constitutive law. Non-homogeneous tests can be used for complex modulus determination only if the behavior is linear viscoelastic. The test methods for each category are summarized below in Table 2.

Table 2. List of stiffness tests for bituminous mixtures

Homogeneous Tests	Non-homogeneous Tests
Tension Compression test	2-point bending
Shearing test	3-point bending
Constant height shearing test	Indirect tensile test
Co-axial shearing test	4-point bending

In the case of viscoelastic materials, their properties are usually presented in the frequency domain as complex numbers having real and imaginary parts. The dynamic modulus can be expressed as

$E^* = \left|E^*\right| \cdot (\cos(\Phi) + i\sin(\Phi))$ (1) where,

Φ is the phase angle between stress and strain cycle [9] ,

and $\left|E^*\right| = \frac{\sigma_0}{\varepsilon_0}$ (2) is the ratio of amplitudes of stress and strain [10]. Further investigation proved that Φ can be defined as $\Phi = \frac{t}{t_p} \cdot 360\ (3)$ [9].

From the previous formulas, dynamic modulus can also be defined with the relations below [10].

$$E_1 = \left|E^*\right| \cdot \cos(\Phi) = \frac{\sigma_0}{\varepsilon_0} \cdot \cos(\Phi)\ (4)$$

$$E_2 = \left|E^*\right| \cdot \sin(\Phi) = \frac{\sigma_0}{\varepsilon_0} \cdot \sin(\Phi)\ \ (5)$$

Commonly, the temperature-frequency or temperature-time superposition principle is being applied in order to produce master-curves [6]. In general, the stiffness modulus decreases with asphalt content and increases with loading frequency. The opposite occurs for the phase angles. The procedure to obtain the master curve is based on the reduced frequency by shifting the given frequency with a shift factor a_t. The shift factor can be calculated using the Arrhenius formula [11].

$\log a_t = C \cdot \left(\frac{1}{T} - \frac{1}{T_{ref}} \right)$ (6), where T is the testing temperature (K) ,

T_{ref} is the reference temperature (K) and
C is a coefficient which is obtained C=10920 K [12], C=13060 K [13] and C=7680 K [14].

In this research, a cyclic tension stiffness test was performed on two replicate samples of each LNRS material at five temperatures (-5°C, 5 °C, 15 °C, 25 °C and 40 °C) and at seven different frequencies namely 0.1, 0.2, 0.5, 1, 2, 5 and 10 Hz. A detailed description of the testing set-up and methodology is given. The obtained results are analyzed and discussed in the next chapter.

4.2.2. Sample preparation

The samples of the three companies were cut in their facilities with predefined dimensions of 30x30x130 mm. However, a further measurement of the beams proved that the accuracy was not precise and the dimensions used for the post-processing of the results were different than the initial ones.

It is worth mentioning that the input of each sinusoidal pulse was computed in order to get approximately 40 points over a period T. For this the width and the number of scans were adapted proportionally. The test setup was a hydraulic testing setup, with two metallic plates and two clamps to ensure a steady and fixed sample.

The samples were glued in the molds with attention in order to avoid bending of the beams. For that reason, special molds to adjust the beams in linearity and parallelism were used (Figure 5). The next step was to bring the samples to the test temperature before applying cyclic loading.

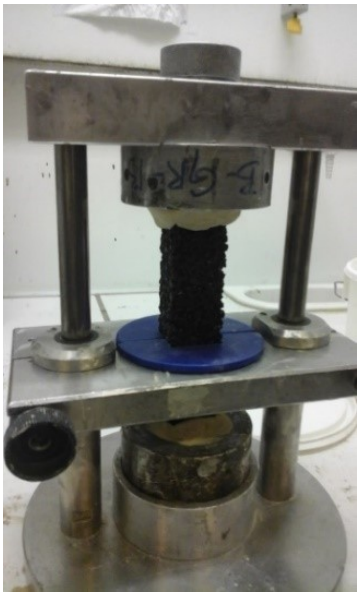

Figure 5. Gluing of the beams in the molds by using two metallic stubs and two 3D plastic molds for alignment

4.2.3. Procedure

All samples were placed in a temperature-controlled chamber, set at the testing temperature, two (2) hours before the execution of the test. Ensuring that the temperature is distributed in the whole mass of the sample, the sample was glued on the loading plates and clamped at the bottom of the hydraulic setup with two clamps (Figure 6).

Next to that, three (3) transducers were placed on the loading plates to calculate the displacement of the beam in correlation with the cyclic load. The range of the linear differential transducers LVDT's was ±5mm in order to give an accurate value of the displacement. The sample with the transducers remained in the UTM hydraulic setup for one more hour before the execution of the test in each specific testing temperature to make sure no temperature losses were created while adjusting the specimen.

Figure 6. Adjusted sample with loading plates, transducers and clampers

The final step was to adjust the preloading and connect the hydraulic setup and measurements of the transducers using software that translates the force and the displacement from Volts to KN and mm, respectively.

4.3. Moisture Sensitivity

4.3.1. Introduction

Moisture damage is a key factor in the design of durable asphalt pavements. The majority of the distress types such as raveling, rutting and cracking are related to the moisture susceptibility of asphalt pavements. In order to estimate these types of distresses three physico-mechanical processes are considered namely: diffusion, erosion and cyclic pore pressure development [15, 16].

The cohesive and adhesive strength of the asphalt mixture are affected significantly during water infiltration. This phenomenon commonly occurs due to long-term diffusion. In contrast, short-term aspects such as dynamic flow phenomena result in cyclic pore pressure which highly affects open-graded asphalt pavement and can cause erosion of the mixture. The main factors that influence this process are the mixture type, the geometry, the air voids and the drainage properties of the mixture [15, 17].

To simulate the aforementioned conditions for the classification of the samples long- and short-term phenomena should be taken into account. Moisture diffusion and pore pressure due to dynamic traffic loading are simulated with a moisture conditioning protocol, in which the samples are initially subjected to bath conditioning and eventually to application of cyclic pore pressure.

Based on past experience of previous projects, moisture affected a lot the durability of LNRS materials. The test method according to NEN-EN 12697-12 [18] used for the evaluation of durability under the dry and moisture condition, is the Indirect Tensile Test (ITT). For the determination of the Indirect Tensile Strength, the following formula is used.

$$ITS = \frac{2P}{\pi DH} \quad [MPa] \quad (7)$$ where,

ITS	is the indirect tensile strength, expressed in MPa, rounded to three significant figures
P	is the peak load, expressed in N, rounded to three significant figures
D	is the diameter of the specimen, expressed in mm, to the third decimal place
H	is the height of the specimen, expressed in mm) to the third decimal place

Finally, the ratio between the strength of wet with dry conditioning is determined as indirect tensile strength ratio (ITSR) by the following formula and is commonly used for the evaluation of the mixture.

$$ITSR = \frac{ITS_{conditioned}}{ITS_{unconditioned}} \times 100 \quad [\%] \quad (8)$$ where,

ITSR	is the indirect tensile strength ratio, in percent (%)
$ITS_{conditioned}$	is the average indirect tensile strength of the conditioned group, in (kPa)
$ITS_{unconditioned}$	is the average indirect tensile strength of the unconditioned group (reference), in (kPa)

To simulate all moisture induced phenomena indirect tensile tests were performed at a variety of conditions. The flexible Material A was tested using direct tensile tests. Firstly, the conditioning procedure that followed in each test is described and afterwards a short description of each test is presented. The results are explained thoroughly in the next chapter.

4.3.2. Testing and moisture conditioning protocol

Bath conditioning was applied to all samples for two (2) and four (4) weeks to simulate the long-term degradation of the material properties. The samples were placed in water baths at a temperature of 60°C to facilitate the infiltration of the water into the samples. The samples were removed from the baths after the specified time and placed at 20°C for two hours for stabilization of the material. The samples were stored afterwards in a chamber at 20°C until they were used for the test.

Figure 7. Bath conditioning of the samples for different time intervals

It is worth mentioning that the standard conditioning method of NEN-EN 12697-12 [18] has the disadvantage of failing to capture the time frame over which moisture infiltration occurs, and furthermore does not take into account the short-term moisture processes related to pumping action. In addition, it has be proven from field observations that stripping of open asphalt mixes is a rather localized phenomenon in trafficked areas of a pavement, which are oversaturated with water [18, 19].

These facts strengthened the claims that pumping action can be an important damage mechanism, and led to the development of the MiST protocol. MiST which stands for Moisture Induced Sensitivity Tester, is a self-contained unit developed by InstroTek that includes a hydraulic pump and a piston mechanism that applies cyclically pressure inside the sample chamber and facilitates the cyclic pore generation [20]. Firstly, the samples are placed in the chamber and filled with water (Figure 8). The water is used to apply the pressure in the compacted sample and consequently creating pressure cycles. It has been chosen to apply 4000 cycles of pressure at a temperature of 60^{o}C and a pressure of 70 psi (480kPa) [20].

Figure 8. MiST device

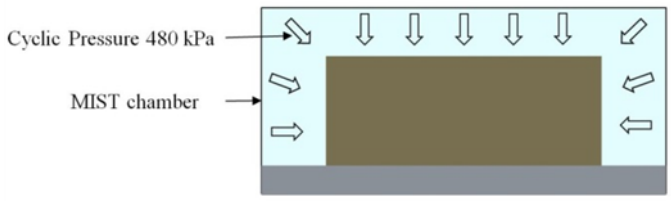

Figure 9. Representation of MiST Conditioning

Totally, three (3) specimens per mixture were used for statistical analysis for each time interval in bath conditioning. In order to compare with dry conditioning three (3) samples were initially stored in the climatic chamber without bath conditioning.

Three (3) specimens per bath conditioning were used for the simulation of traffic and time conditions in MiST. Moreover, the dry specimens were used also for MiST. After the procedure of MiST, the specimens are again placed in water for two (2) hours at 20°C and then stored in climatic chamber until the test [20]. An overall schematic representation of the moisture conditioning protocol is given in Figure 10.

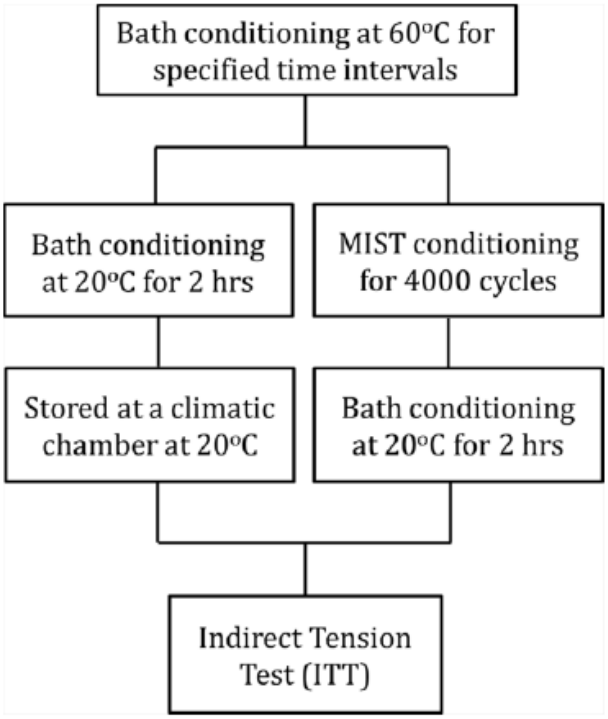

Figure 10. Schematic representation of moisture conditioning protocol

4.3.3. Procedure

4.3.3.1. Indirect Tensile Test (ITT)

The LNRS cylindrical samples had a diameter of 100 mm and a thickness of 30 mm. In total, eighteen (18) specimens for each LNRS material were used, three (3) specimens per conditioning interval. The conditioning intervals, were two (2) and four (4) weeks of bath conditioning and dry conditions. For simulation of pore pressure, after applying the same bath conditions of zero (0), two (2) and four (4) weeks, MiST conditioning was performed. It was already known that the LNRS samples of Material A was too flexible to crack in ITT and an alternative of a direct tensile test were used for this material. According to EN12697-23 [22] the test is carried out at a temperature of 20°C at a loading rate of 50,8mm/min.

The machine as well as all the test specimens were already placed in the test temperature two (2) hours before the beginning of the test to provide beforehand homogeneous distribution of the temperature in the depth of the whole sample. Moreover, the specimens should be tested immediately after putting out of the chamber test temperature in order to manage equal conditions for all the tested specimens. With this test, the maximum tensile stress which is applied through compression of the cylindrical specimen until failure is computed. During the test, the cylindrical specimen is correctly aligned between the loading strips, with 12.7 mm width, of the apparatus and then the load is applied diametrically along the direction of the cylinder axis with a constant speed of displacement until cracking of the specimen. By using the accurate dimensions of the specimen, the maximum tensile stress can be calculated.

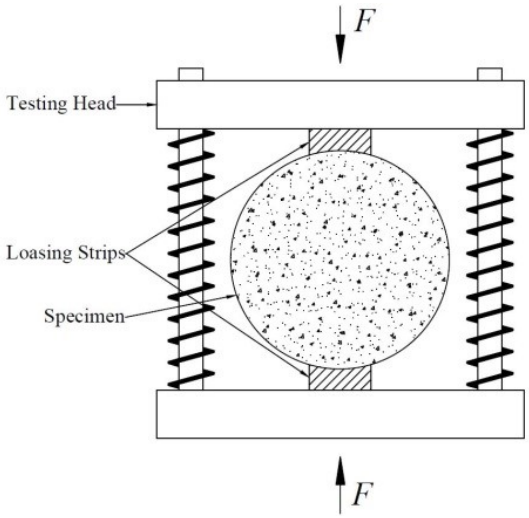

Figure 11. Schematic scheme of ITT

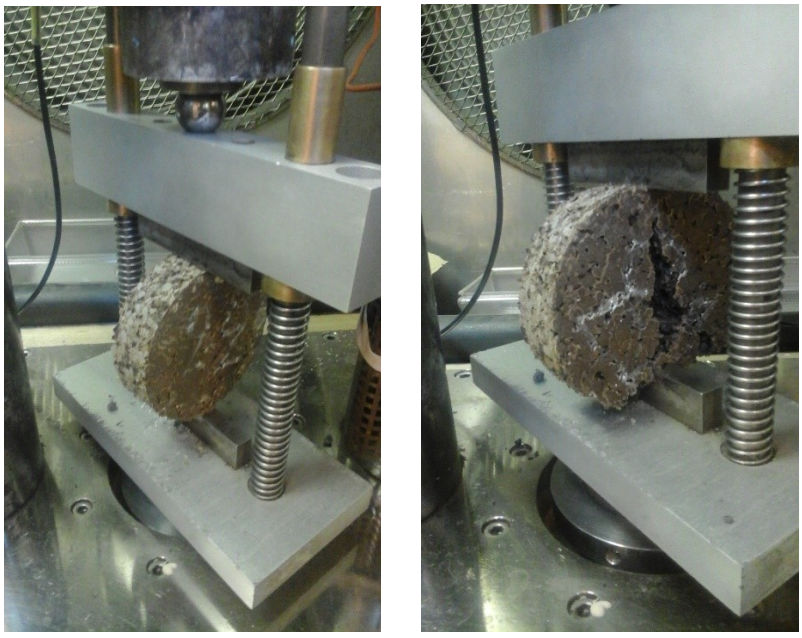

Figure 12. Sample before and after the ITT test

4.3.3.2. Direct Tensile Test (DTT)

Material A was too flexible to fail in ITT and it returned to its initial shape after removing the load. To make an equal comparison between all the samples from the three companies a direct tensile test after application of the conditioning in the cylindrical samples was performed. The cylindrical samples were sawn in small beams with dimensions 30x30x80 mm according to NEN12697-46 [23].

The sawing of the beams was as much as accurate because the material was not easily cut due to the existence of rubber in the specimen of Material A.

Figure 13. Sawing of the beams from the cylinder sample.

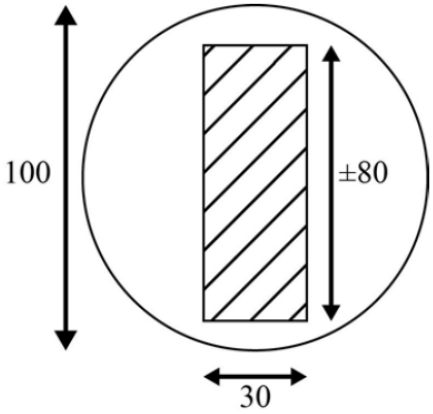

Figure 14. Dimensions of the beams

After that, the beams were glued with a special apparatus in metallic caps and placed in the machine which has a hydraulic testing setup and two hinges were the beams with the caps were placed. It is worth mentioning that special plastic pieces, created with a 3-D printer were placed in the corner between the cap and the specimen to avoid cracking in this area and adhesive failure and provide better bonding. All the beams glued in the caps were placed in a climatic chamber at 20^{o}C two hours before the test as well as the testing machine. The vertical displacement rate was adjusted in such a way to make a fair comparison between ITT and DTT. The speed applied was 14.6mm/min similar to ITT as explained further in an analysis of the results. The applied load and displacement was measured until cracking of the specimen. The measured maximum force divided by the cross sectional area gives the desired strength value of the sample.

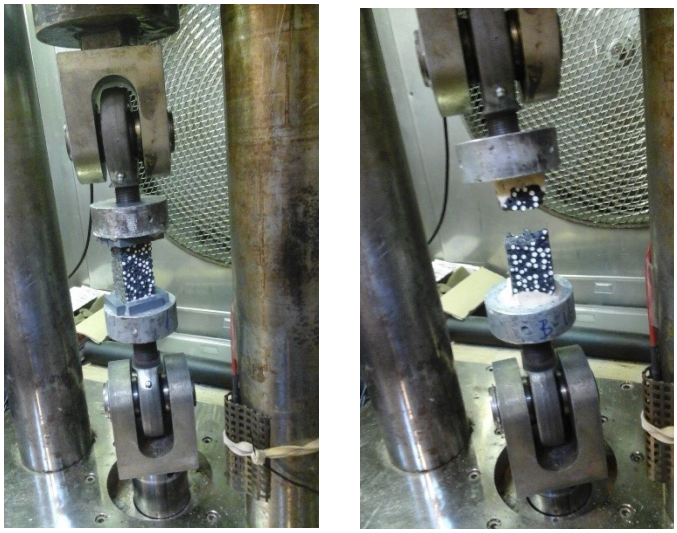

Figure 15. Material A before and after the DTT test

4.4. Interlayer Bonding

4.4.1. Introduction

Not only the material properties of each individual layer, but also the interlayer bond play an important role in achieving a long-term structural performance of a pavement. Bond strength is extremely important for the bearing capacity and developed the adhesion testing methods as subject of study during the recent years. The complexity of the influencing parameters for the interaction of the layers such as aggregate size, binder properties and mixture composition, made the qualitative requirements for the bond more difficult [24]. This type of damage appeared also in most of the previous projects with LNRS materials. The most commonly used methods for the estimate of interlayer bond are presented in Table 3.

Table 3. List of bond strength tests for bituminous mixtures

Homogeneous Tests
Leutner shear test
Wedge Splitting test (Indirect tensile)
Torsion test
Pull-off test (tensile test)

It is worth mentioning that there is not yet a specification that describes the procedure for the evaluation of the interlayer bonding among the different layers. As can be seen in Table 3 a lot of different methods have been proposed to determine the bond. Eventually the choice depends on the loading mode, the type of application, the problem area and the repeatability of the test method [24].

Some of the main distress types, which appeared in previous LNRS projects, are due to the presence of water [25]. Among the other distress types, water highly affects the bond and glue of the surface with the base course.

Further investigation was performed on the bond strength and specifically the bonding of ZOAB-layer below them with the three (3) different LNRS materials from each company. The presence of moisture between the layers affects highly their bond and results in adhesive failure. Uniaxial tensile tests are performed to investigate this bond strength not only at dry conditions but also after bath conditioning. Usually different moisture conditions are investigated for the bond strength and commonly used evaluation is based on the determination of adhesive strength ratio (ASR) between dry and wet conditions.

The ASR is calculated as follows

$$ASR(\%) = \frac{BondStength_{wet}}{BondStrength_{dry}} \times 100[\%] \quad (9)$$

The results presented in Chapter five are being used to calculate the peak force and strength. The bath conditioning intervals of two (2), four (4) and six (6) weeks are used. To make a fair comparison the bond strength of the LNRS materials should be compared with two-layer ZOAB (PA), which is the standard wearing course for the Dutch highways.

4.4.2. Testing and moisture conditioning protocol

The specimens were cored from a slab of two layers with 30mm LNRS material above and 50mm ZOAB underneath. In total, twelve (12) cores with a 50 mm diameter were tested. All specimens were measured their dimensions, which were used in the computation of bond strength. The next step was to place the specimen in bath conditioning to simulate the water damage in real application and the loss of bond strength with time. The bath temperature was fixed at 60^{o}C following the same protocol as for moisture sensitivity tests. After two (2), four (4) and six (6) weeks three (3) specimens were put out of the baths stored in wooden buckets filled with sand in a climate chamber (Figure 16). After one week, a special wooden apparatus was used to glue the specimens onto the metallic pulling stubs in proper alignment. Afterwards, the samples were clamped at the testing machine. The apparatus and the special 3D rings, which were used to create a pool of glue and avoid the failure at the ends of the sample in the pull stab interface, are shown in Figure 17. By using these rings, the glue was concentrated in a bigger area along the height of the specimen providing the proper strength between the specimen and the stub.

Figure 16. The glued specimens stored on sand-layer in a climate chamber

Figure 17. The apparatus used for alignment and the 3-D rings

4.4.3. Procedure

The next step was to place the samples at the testing temperature of 20°C two hours before the execution of the test. The vertical displacement was adjusted in 50.8mm/min similar to moisture sensitivity tests. The applied load was measured until cracking which was expected in the interface. The test was carried out using a testing setup, which included a climate chamber and a pneumatic single axis frame.

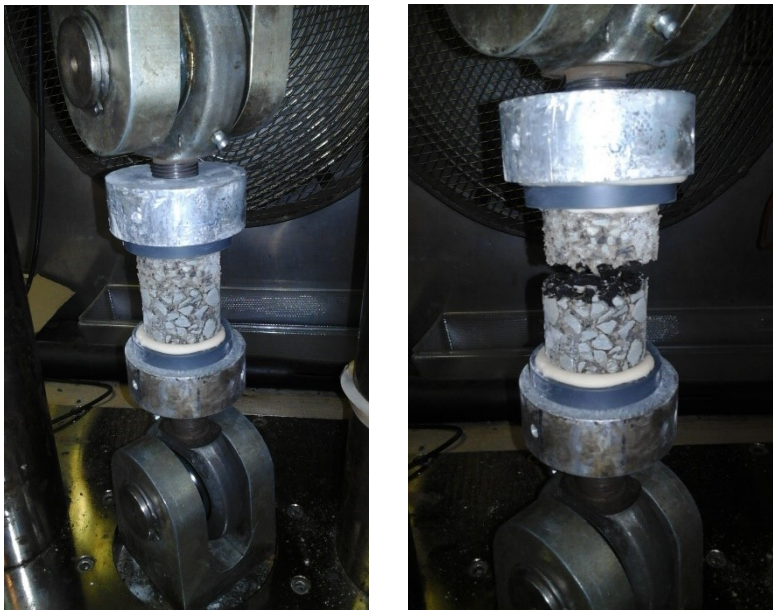

Figure 18. Sample before and after the interlayer bonding test

5. Test results analysis

5.1. Stiffness Test

5.1.1. Data analysis and results

In order to estimate the dynamic modulus and phase angle of each material stiffness tests at different temperatures and frequencies were performed. The well-known formula (1) of the dynamic complex modulus could be used to estimate the value of each material, however noise should be eliminated from the sinusoidal pulse and for that reason this procedure is considered inaccurate. Instead, a normalized Fast Fourier Transformation (FFT) was applied to evaluate the crucial properties of stiffness test [26]. If noise phenomena are taken into account, our raw data seems rather far away from its sinusoidal behavior.

Taking into account the noise introduced in the sinusoidal applied force, a (FFT) Matlab algorithm was used, in order to isolate the desired frequency for which the fundamental properties of complex dynamic modulus and phase angle are investigated. For better normalization of the given sinusoidal the frequency introduced step in Matlab was calculated such as to export accurate value of the given frequency each time.

By making use of FFT the given signal is translated in the frequency domain and after that focus was placed on the examined frequency that was the governing one. This can be easily depicted in an amplitude frequency response graph as depicted below (Graph 2). The governing frequency in a FFT is the given initial frequency ignoring noise frequencies. For that specific frequency the complex dynamic modulus and phase angle are calculated.

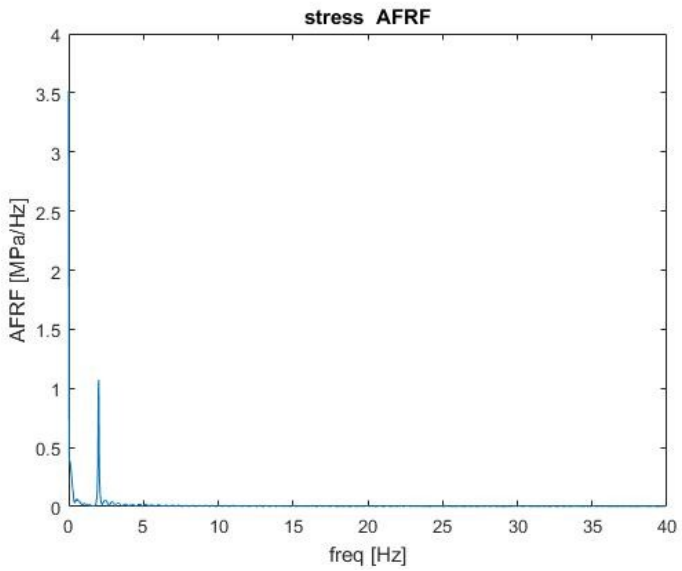

Graph 2. Example of amplitude-frequency response function at 2 HZ with FFT

As mentioned above, the raw data were normalized through FFT and the phase angle was exported for the given governing frequency of the application of the load each time. In that way noise effects and inaccuracy of the imperfection of sine waves was avoided. For the computation of the stress and strain, the force was divided with the upper area of the beam and multiplied by a factor to translate Volts in MPa.

Moreover, the average displacements of the three (3) transducers was divided with the actual length of the beam, multiplied with a specific factor to translate Volt into mm and eventually resulted in the strain, which as expected is dimensionless. The amplitude of the dynamic modulus was obtained as the ratio between stress and strain expressed in MPa. For the phase angle, Matlab exported the result through FFT as the phase lag between the two sinusoidal waves of stress and strain eliminating noise effects. The results for the three (3) different companies are depicted in Tables 4-6.

Table 4. Dynamic modulus and phase angle of Material A

Sample		Sample A 1		Sample A 2	
Temperature (°C)	Frequency (Hz)	Phase angle (°)	Dynamic Modulus (MPa)	Phase angle (°)	Dynamic Modulus (MPa)
-5.0	10.0	6.6	50.5	6.1	51.3
	5.0	6.7	48.4	6.4	48.7
	2.0	6.7	44.5	7.0	46.0
	1.0	7.5	41.1	7.1	42.4
	0.5	8.6	39.2	7.2	40.8
	0.2	11.3	37.5	10.9	38.1
	0.1	12.6	33.1	11.8	34.8
5.0	10.0	5.5	38.0	5.4	39.8
	5.0	7.8	34.9	6.4	36.9
	2.0	8.0	32.0	6.5	34.7
	1.0	8.3	30.1	7.9	32.5
	0.5	8.3	29.1	8.8	33.2
	0.2	8.4	28.0	9.1	31.4
	0.1	8.8	27.9	11.5	30.1
15.0	10.0	4.8	30.2	4.7	32.2
	5.0	5.0	28.9	5.5	30.8
	2.0	7.8	26.4	8.1	29.0
	1.0	8.8	26.3	8.4	27.4
	0.5	9.3	25.4	8.5	25.7
	0.2	10.5	23.5	8.5	25.2
	0.1	11.9	23.2	8.6	23.8
25.0	10.0	3.5	27.0	3.7	29.5
	5.0	3.6	25.3	4.3	27.0
	2.0	4.1	24.3	5.5	24.3
	1.0	5.4	23.5	6.0	23.7
	0.5	6.3	22.8	6.1	22.5
	0.2	7.4	20.7	7.7	21.8
	0.1	8.9	20.9	7.7	21.9
40.0	10.0	4.8	22.1	3.2	25.3
	5.0	6.0	22.2	4.1	23.0
	2.0	6.8	19.7	5.7	22.1
	1.0	7.1	19.5	6.0	21.3
	0.5	8.3	18.4	8.7	21.2
	0.2	8.3	17.2	8.8	19.6
	0.1	8.9	17.1	9.4	18.7

Table 5. Dynamic modulus and phase angle of Material B

Sample		Sample B 1		Sample B 2	
Temperature (°C)	Frequency (Hz)	Phase angle (°)	Dynamic Modulus (MPa)	Phase angle (°)	Dynamic Modulus (MPa)
-5.0	10.0	5.8	773.3	5.7	808.8
	5.0	6.0	752.6	5.8	769.4
	2.0	6.0	705.3	5.9	756.1
	1.0	6.1	690.1	6.0	743.1
	0.5	6.2	675.6	6.0	711.4
	0.2	6.2	646.9	6.3	666.5
	0.1	6.5	609.4	6.7	644.1
5.0	10.0	5.1	679.9	5.7	639.3
	5.0	8.7	612.8	5.8	604.3
	2.0	8.8	582.9	5.8	584.2
	1.0	9.1	559.7	5.9	580.6
	0.5	8.8	537.2	6.0	557.5
	0.2	9.1	531.7	6.2	508.2
	0.1	9.5	487.8	6.4	504.0
15.0	10.0	6.5	521.8	5.9	575.6
	5.0	6.7	480.6	6.0	540.5
	2.0	6.8	456.7	6.0	512.2
	1.0	6.8	420.5	6.9	509.5
	0.5	7.5	422.4	7.0	488.3
	0.2	13.2	402.7	12.0	452.3
	0.1	15.6	384.7	14.7	441.4
25.0	10.0	5.8	468.6	5.8	472.7
	5.0	5.8	452.8	5.8	469.3
	2.0	5.9	442.5	5.9	459.2
	1.0	6.1	412.7	6.1	449.5
	0.5	6.2	398.8	6.2	390.9
	0.2	6.2	390.4	7.3	413.3
	0.1	7.2	375.9	7.7	372.9
40.0	10.0	6.0	354.9	5.5	383.4
	5.0	6.9	345.9	5.9	367.6
	2.0	7.0	343.7	5.9	350.6
	1.0	7.1	328.6	6.1	342.9
	0.5	7.3	317.7	6.2	340.2
	0.2	7.4	307.2	6.5	311.7
	0.1	8.2	305.9	7.1	307.6

Table 6. Dynamic modulus and phase angle of Material C

Sample		Sample C 1		Sample C 2	
Temperature (°C)	Frequency (Hz)	Phase angle (°)	Dynamic Modulus (MPa)	Phase angle (°)	Dynamic Modulus (MPa)
-5.0	10.0	4.0	2987.2	4.2	2918.2
	5.0	4.3	2849.8	4.5	2807.4
	2.0	4.3	2790.2	4.8	2679.9
	1.0	4.5	2573.0	5.1	2469.2
	0.5	4.7	2419.6	5.8	2352.9
	0.2	5.6	2249.5	6.0	2187.4
	0.1	5.8	2152.4	6.1	2057.8
5.0	10.0	4.8	2261.4	3.8	2098.6
	5.0	5.1	2190.8	3.6	1987.2
	2.0	6.5	2086.1	4.0	1854.7
	1.0	6.8	1894.0	5.7	1707.2
	0.5	18.1	1561.3	15.2	1648.0
	0.2	19.3	1360.8	16.1	1565.0
	0.1	20.2	1124.2	17.4	1267.1
15.0	10.0	12.7	1837.1	12.5	1940.5
	5.0	14.3	1787.0	12.5	1770.4
	2.0	14.7	1332.6	13.8	1388.7
	1.0	26.3	1123.1	21.5	1160.3
	0.5	32.2	1093.4	29.6	1144.0
	0.2	37.3	962.5	33.3	945.5
	0.1	40.2	826.2	37.4	913.1
25.0	10.0	19.4	1104.7	27.2	943.3
	5.0	21.2	937.1	30.9	652.2
	2.0	23.6	762.0	32.1	442.5
	1.0	30.6	675.1	34.8	351.3
	0.5	30.9	443.1	36.9	324.2
	0.2	38.0	308.2	39.8	252.6
	0.1	42.6	226.7	43.0	233.4
40.0	10.0	11.9	302.8	12.3	351.3
	5.0	16.2	228.0	16.0	235.7
	2.0	20.6	195.5	16.3	185.1
	1.0	23.2	153.4	22.1	157.4
	0.5	25.1	122.6	24.6	134.5
	0.2	30.5	93.7	28.9	102.7
	0.1	32.9	81.7	33.4	92.3

5.1.2. Discussion of the results

In order to compare the differences between the LNRS materials the master curves were plotted with a reference temperature of 15°C according to formula (6). The initial value of the shift factor was further adapted in order to obtain smoother master curves.

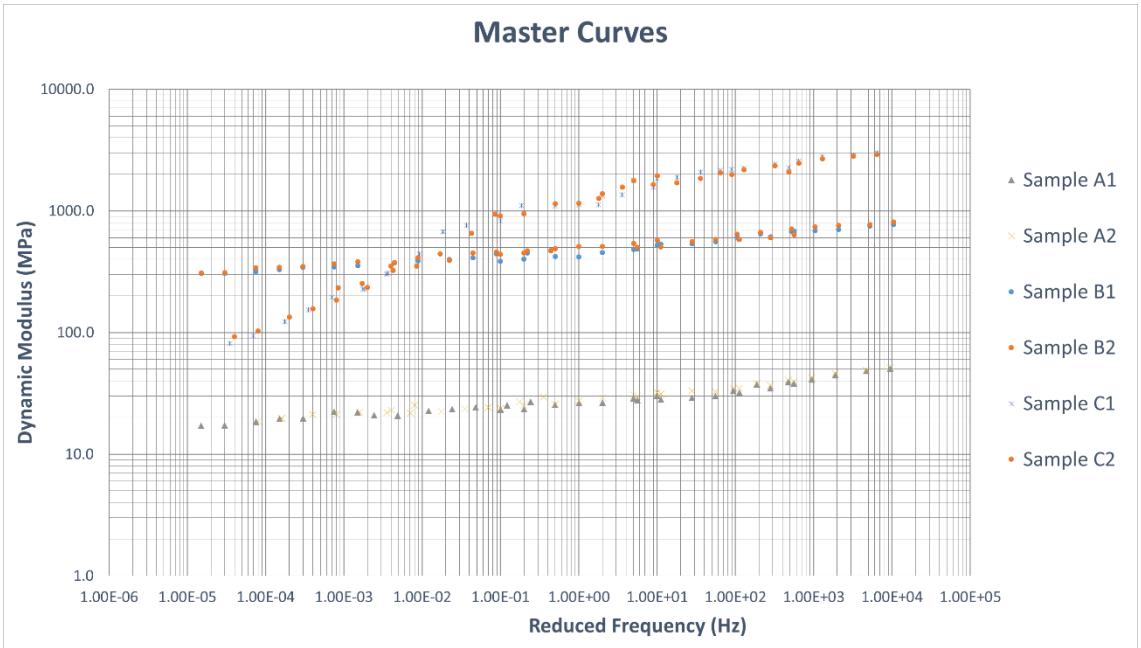

Graph 3. Cumulative graph of the master curves

Graph 3 shows the master curves of the three LNRS materials. It can be observed that Material C has the higher stiffness whereas the Material A is the most flexible one. Material A has the lowest stiffness, which could be justified by the high percentage of rubber in the mixture which leads to high elasticity. The trend of Material A looks rather steady during the increase of frequencies. On the other hand, Material C experiences a sharp increase in the stiffness for higher frequencies (low temperatures) apparently due to lack of rubber in the mixture. The stiffness of Material B steadily increases with increasing frequency and the range of its values is between the values of the other two materials. From Graph 3, we easily observe that Material C has higher values for the higher frequencies over 0.01 Hz, whereas for lower values of frequency Material B has higher stiffness. Material A has low stiffness in the whole frequency range.

For Material A, the phase angle values increase to some extent with increasing frequency at a specific temperature, whereas the phase angle values of the Material B does not change considerably at different temperatures or frequencies. Overall, the results of Tables 4 and 5 suggest that both mixtures have low susceptibility to temperature. Finally, Table 6 shows that the phase angle values of the Material C increase with increasing temperature (or decreasing frequency), indicating that the mixture is temperature susceptible.

5.2. Water Sensitivity

5.2.1. Data Analysis and Results

The results given initially in Volts were multiplied by a coefficient to translate into mm and KN. Typical graphs of force over time for each material were plotted presenting peak force of cracking for each material. From these graphs it is easily observed the brittle behaviour of Material C comparing to Material A and B.

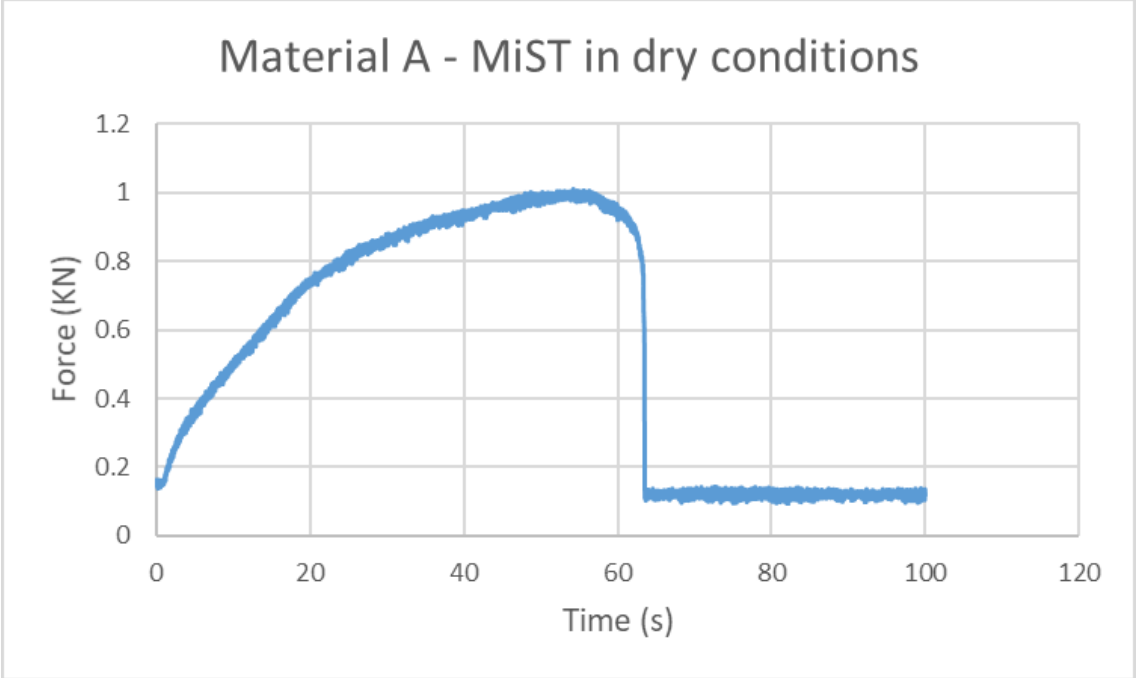

Graph 4. Typical graph of elongation and force of Material A

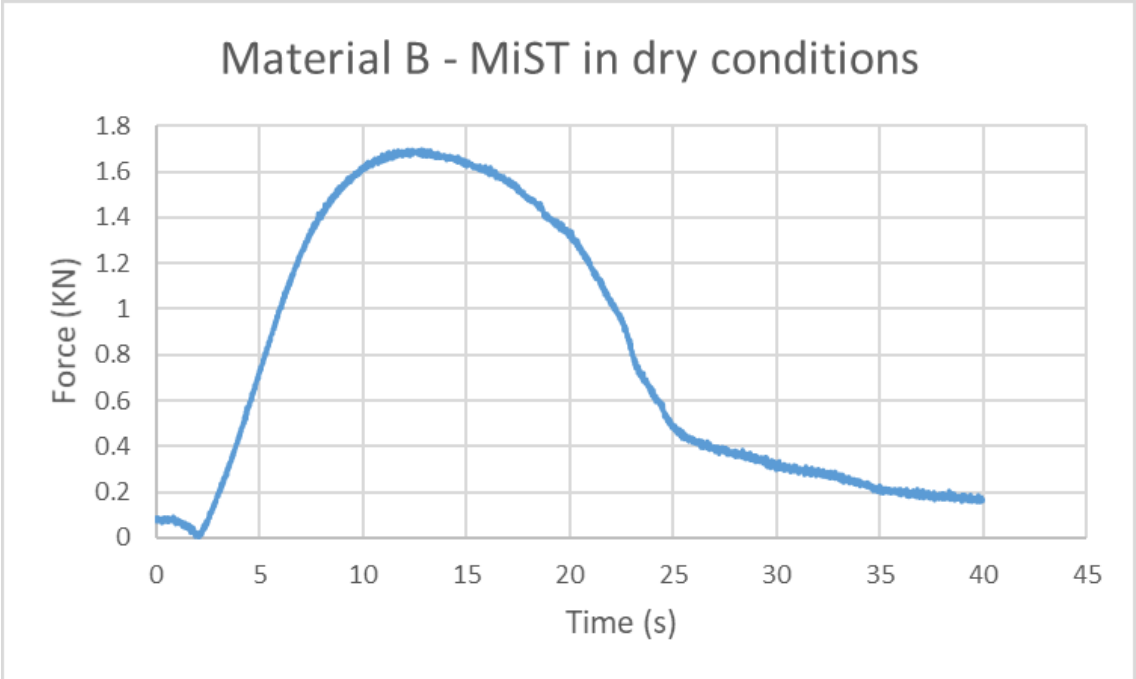

Graph 5. Typical graph of deformation and force of Material B

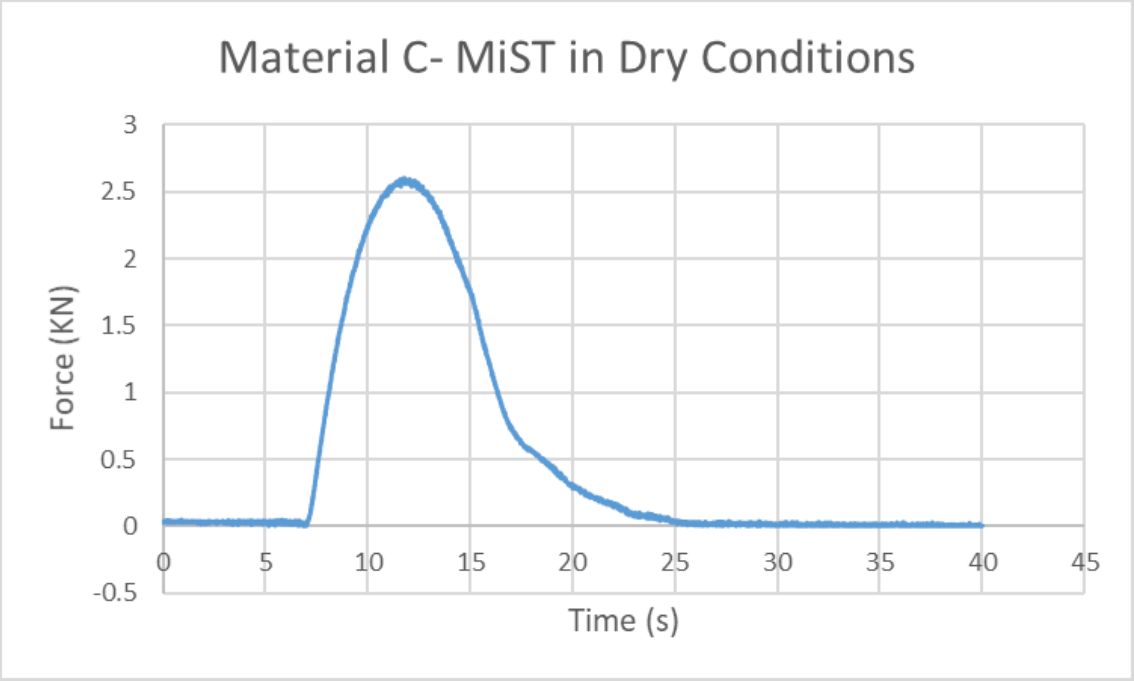

Graph 6. Typical graph of deformation and force of Material C

Material A could not be tested using an indirect tensile test because of its high elasticity and therefore a DTT was performed. Using the useful results from previous research, which related the displacement speed between ITT and DTT tests, a comparison of the indirect tensile test results with that of direct tensile test was achieved [27].
The strain rate of the DTT, if the specimen cross section is constant over the specimen height, can be found by dividing the deformation rate by the specimen height expressed as

$$\dot{\varepsilon} = \frac{\dot{u}}{h} \quad (10)$$

However, during the indirect tension test the loading direction is perpendicular to the direction in which failure occurs. The internal stress distribution is extremely complicated and the deformation along the vertical axis can be calculated on the basis of the following equation

$$u_y = \int_{-R}^{R} \varepsilon_y dr = \frac{1}{E} \int_{-R}^{R} (\sigma_{ry} - v \cdot \sigma_{\theta y}) dr \quad (11)$$

, where
ε_y = strain in the vertical direction,
E = Young's Modulus
v = Poisson's ratio
u_y = total specimen deformation along the vertical axis

For the ITT assuming a Poisson's ratio of 0.33 with specimen diameter 100mm and thickness t=25mm after integration $\dot{\varepsilon}_x = 0.0036 \cdot \dot{u}_y$ (12) is derived, simulating the perpendicular direction of cracking [27].

Using the displacement rate of ITT equal to 50.8mm/min for a height of 80mm, a deformation rate for DTT equal to 14.6mm/min can be calculated as shown in the following

$$0.0036 \cdot \dot{u}_y = \frac{\dot{u}}{h} \Leftrightarrow 0.0036 \cdot 50.8 = \frac{\dot{u}}{80} = 14.6\left[mm/\min\right]$$

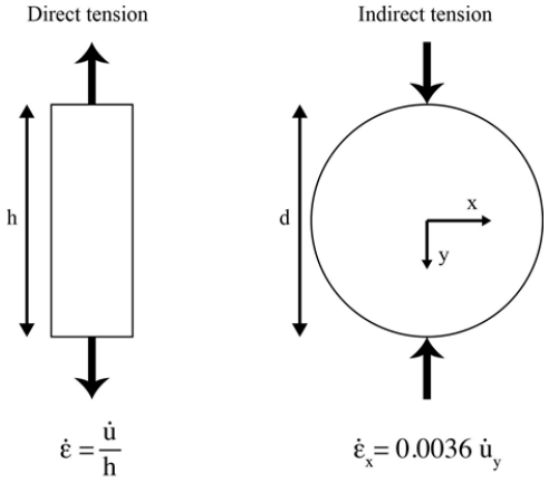

Figure 19. Comparison between DTT and ITT

The DDT results were then adjusted further using statistical analysis between the results of uniaxial tensile tests and indirect tensile tests as presented in previous research work [26]. Assuming a similar behaviour of the LNRS materials during the DTT and the ITT tests, we use the results presented in Graph 7 to account for the differences in strength values between the two tests. Therefore, the initial data of the DTTs were decreased by 15%, as shown in the Graph 7 for a strain rate of 0.3%/s and a testing temperature of 20°C. [28].

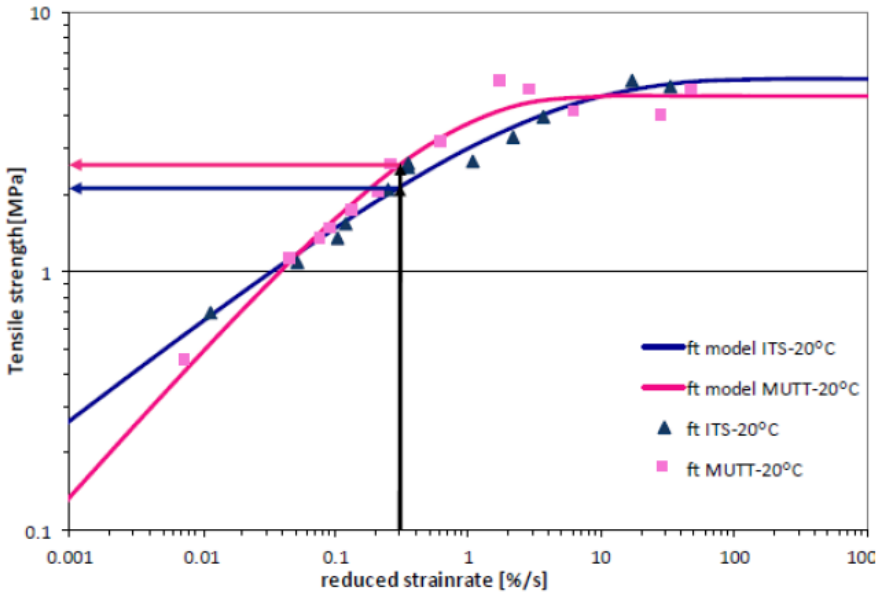

Graph 7. Master curve for ITT and DTT based on previous research and the difference for a strain rate of 0,3%/s [28]

The results are presented in Table 7 and further plotted in Graphs 8-10. For each conditioning 3 replicate samples per material were tested. An indication of the repeatability of each sample is shown by computing the standard deviation and the coefficient of variation for each conditioning.

Table 7. Tensile strength for all LNRS mixtures

Company	Conditioning	Number of repetitions	Mean ITS (MPa)	Standard deviation σ (Mpa)	CV (%)
Material A	Dry	3	0.738	0.040	5.381
	Dry and MiST	3	0.769	0.054	7.037
	2 weeks in bath	3	0.814	0.009	1.157
	2 weeks in bath and MiST	3	0.835	0.030	3.572
	4 weeks in bath	3	0.608	0.049	8.062
	4 weeks in bath and MiST	3	0.601	0.022	3.727
Material B	Dry	3	0.776	0.029	3.676
	Dry and MiST	3	0.334	0.022	6.723
	2 weeks in bath	3	0.327	0.002	0.644
	2 weeks in bath and MiST	3	0.304	0.009	2.999
	4 weeks in bath	3	0.361	0.020	5.437
	4 weeks in bath and MiST	3	0.293	0.013	4.358
Material C	Dry	3	0.935	0.062	6.645
	Dry and MiST	3	0.585	0.035	6.050
	2 weeks in bath	3	0.944	0.028	2.919
	2 weeks in bath and MiST	3	0.875	0.046	5.229
	4 weeks in bath	3	0.723	0.028	3.858
	4 weeks in bath and MiST	3	0.759	0.039	5.113

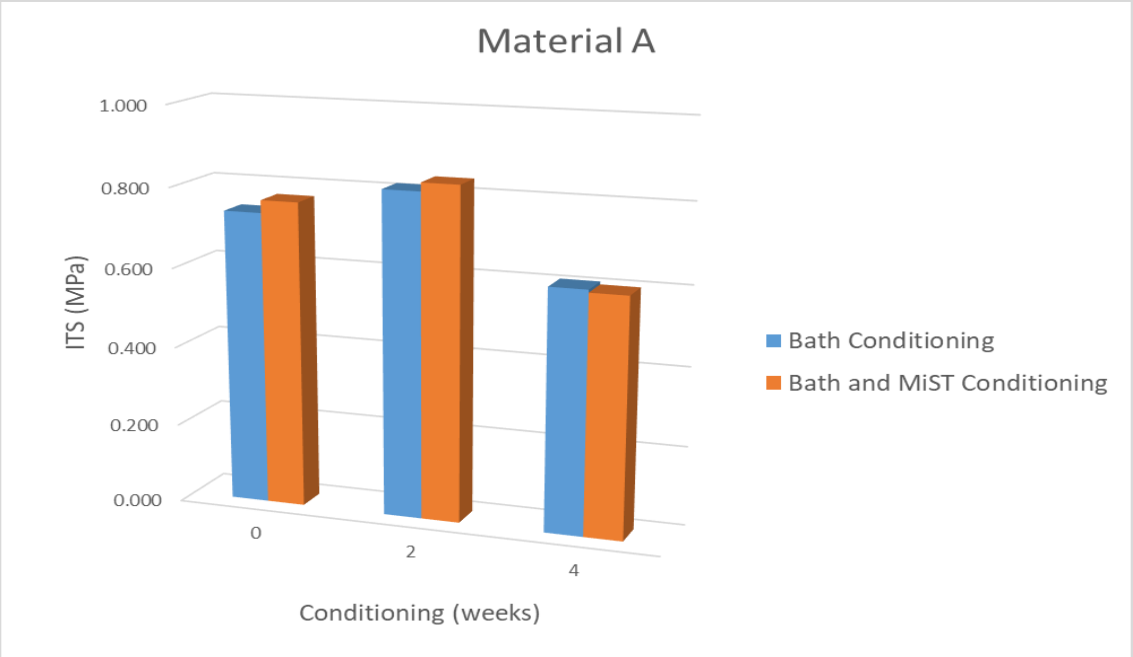

Graph 8. ITS for Material A

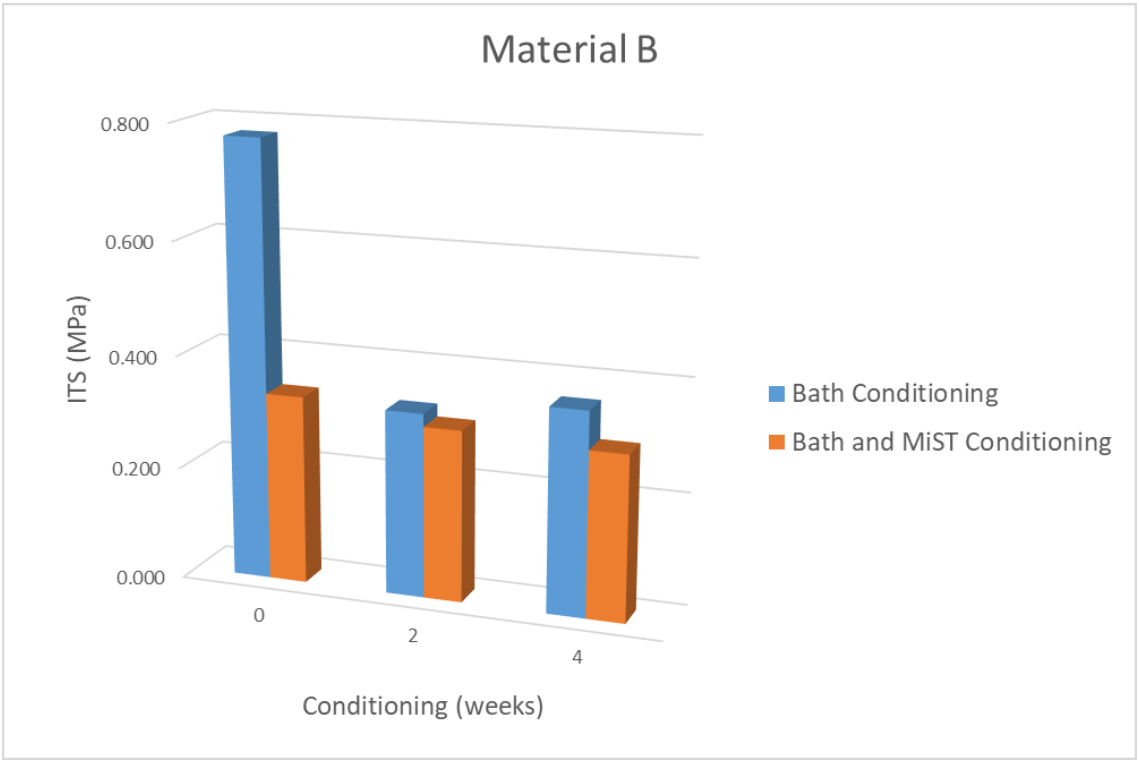

Graph 9. ITS for Material B

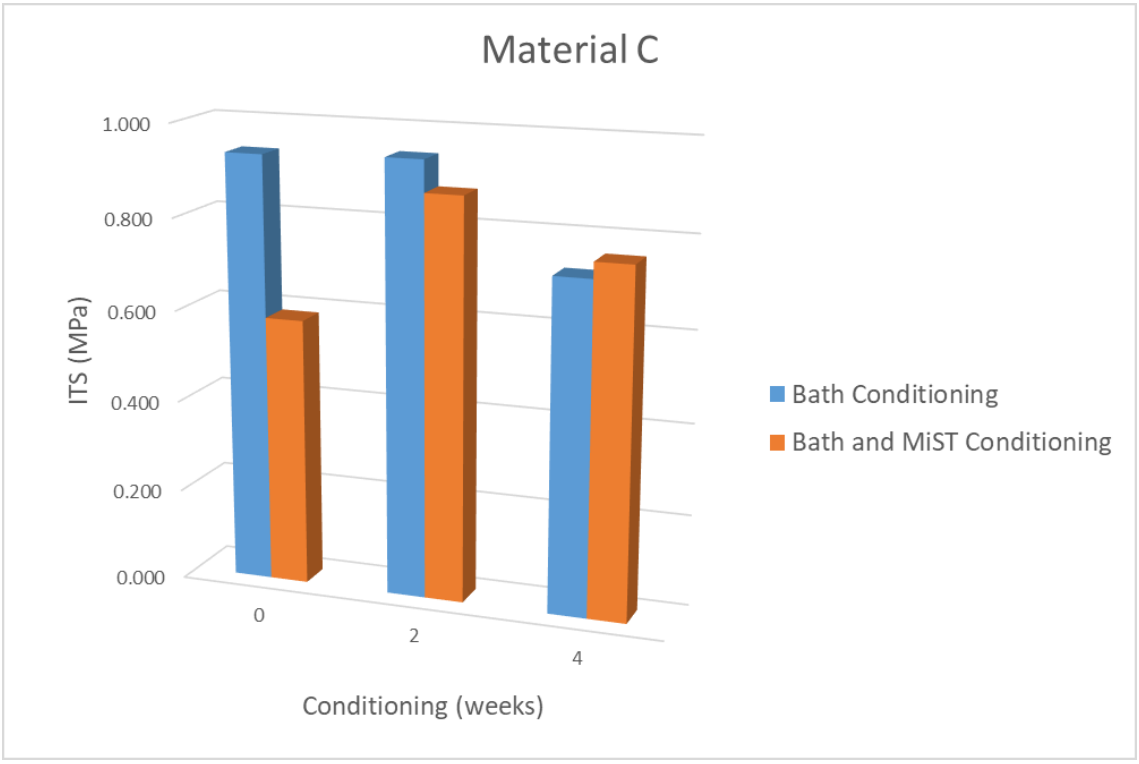

Graph 10. ITS for Material C

Furthermore, the ITSR is computed according to formula (8). The results are presented in Table 8.

Table 8. ITSR values for the 3 materials

Company	Conditioning	ITSR (%)
Material A	Dry	100.00
	Dry and MiST	104.30
	2 weeks in bath	110.33
	2 weeks in bath and MiST	113.25
	4 weeks in bath	82.42
	4 weeks in bath and MiST	81.48
Material B	Dry	100.00
	Dry and MiST	43.08
	2 weeks in bath	42.09
	2 weeks in bath and MiST	39.18
	4 weeks in bath	46.47
	4 weeks in bath and MiST	37.79
Material C	Dry	100.00
	Dry and MiST	62.58
	2 weeks in bath	100.95
	2 weeks in bath and MiST	93.60
	4 weeks in bath	77.36
	4 weeks in bath and MiST	81.15

5.2.2. Discussion of the results

An evaluation of the moisture damage of the materials could be done for the different conditioning protocols. For Material A, an increase in the time of bath conditioning and applying afterwards pore pressure simulation increases slightly the indirect tensile strength of the LNRS Material A. The high flexibility of Material A, as observed by the stiffness tests, causes the mixture to be insensitive to the application of pore pressure cycles. On the other hand, Material B is highly susceptible to moisture. Both the application of pore pressure and bath conditioning decreases dramatically the strength of the mixture. Finally, Material C exhibits an upward trend over time with both conditioning types at two (2) weeks and decreases again for four (4) weeks in the two types of conditioning. Pore pressure application influences more the material. This can be attributed mainly to the high stiffness of the material, which does not allow the redistribution of the internal pressure-induced stresses, and therefore leads to damage of the material. However, a combination of bath conditioning and MiST application causes a change in the performance of the mixture, as the influence of pore pressure application is not that significant. This change in performance can be explained possibly by the softening effect of water on the binder of the Material C that reduces the overall stiffness of the material and results in a less stiff mixture that can sustain a larger number of pore pressure cycles.

Taking into account the Dutch specifications of NEN 12697-12 [18] a mixture is considered susceptible to moisture if the value meets the criterion for the indirect tensile strength ratio higher than 80%. From Table 8 can be easily observed that Material A fulfils this requirement,

as well as Material C (except from the case when MiST is applied without bath conditioning). Material B shows poor susceptibility to moisture after both short- and long-term conditioning and does not fulfil the Dutch standards for moisture susceptibility.

5.3. Interlayer bonding

5.3.1. Data Analysis and Results

For the computation of the results, using the measured dimensions of the samples and divide the recorded maximum force by this area, a strength value is calculated. Afterwards typical graphs of displacement and elongation are plotted for each Material of the three companies. We can easily observe brittle failure for Material B and C and higher force values for Material C.

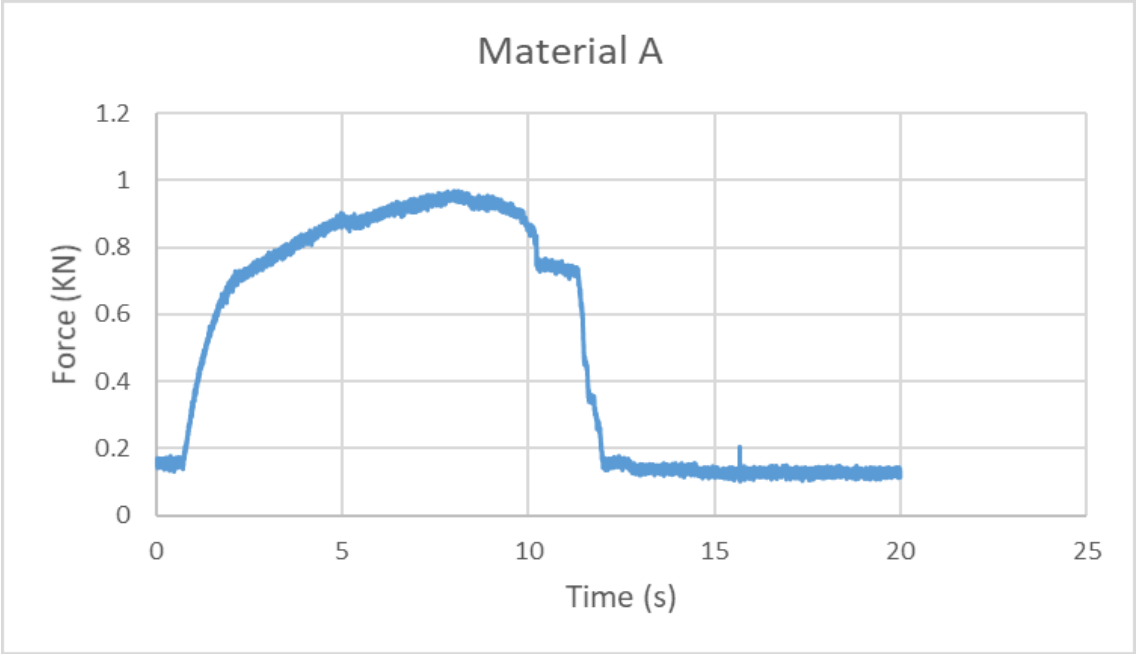

Graph 11. Typical graph of bond strength of Material A

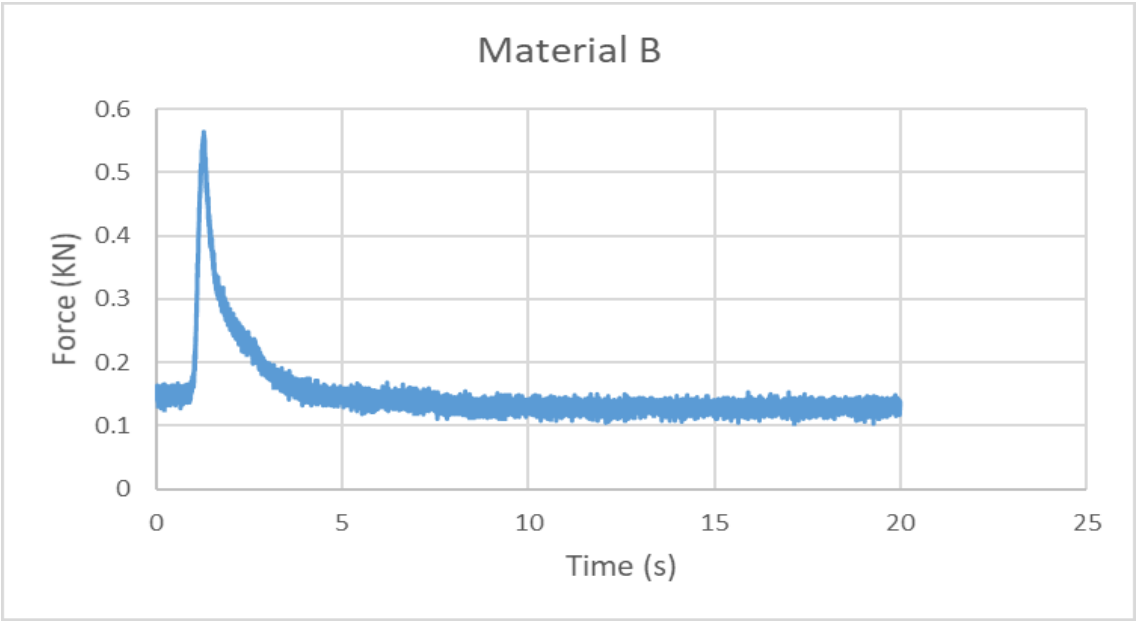

Graph 12. Typical graph of bond strength of Material B

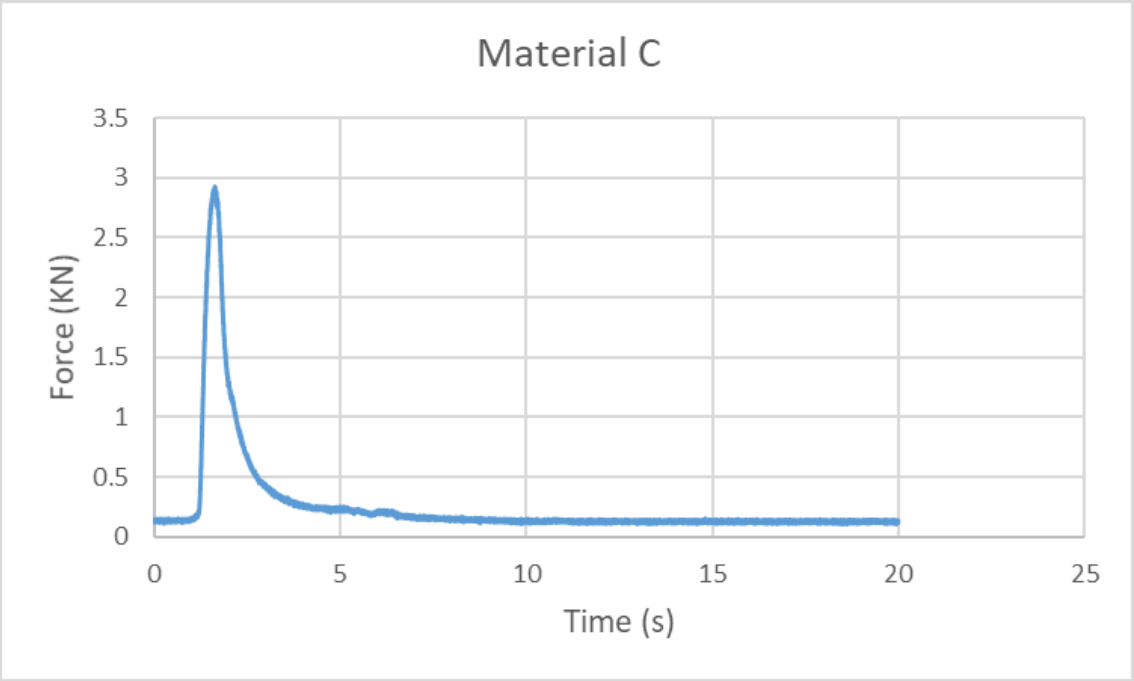

Graph 13. Typical graph of bond strength of Material C

The results for each material are presented in Table 9. In the same table the values of two references ZOAB systems are presented, namely a two-layer porous asphalt with a 4/8 top layer on a 11/16 bottom layer and another fine graded two-layer porous asphalt with a 2/6 top layer on an 8/11 under layer. Four (4) specimens for each ZOAB system were tested as to obtain the reference values.

The gradation 2/6-8/11 used is comparable with the LNRS mix designs in development. Graph 14 illustrates the degradation of bond strength with bath conditioning time for the USW and reference materials.

Table 9. Bond strength of the 3 LNRS materials and the 2 reference materials

Adhesive bond strength (Mpa)	Number of repetitions	Dry	2 weeks	4 weeks	6 weeks
Material A	3	0.75	0.75	0.53	0.54
Material B	3	1.22	0.27	0.21	0.22
Material C	3	1.48	1.32	1.13	0.77
ZOAB(2/6 - 8/11)	3	0.82	0.82	0.62	0.42
ZOAB(4/8 - 11/16)	3	0.71	0.72	0.51	0.35

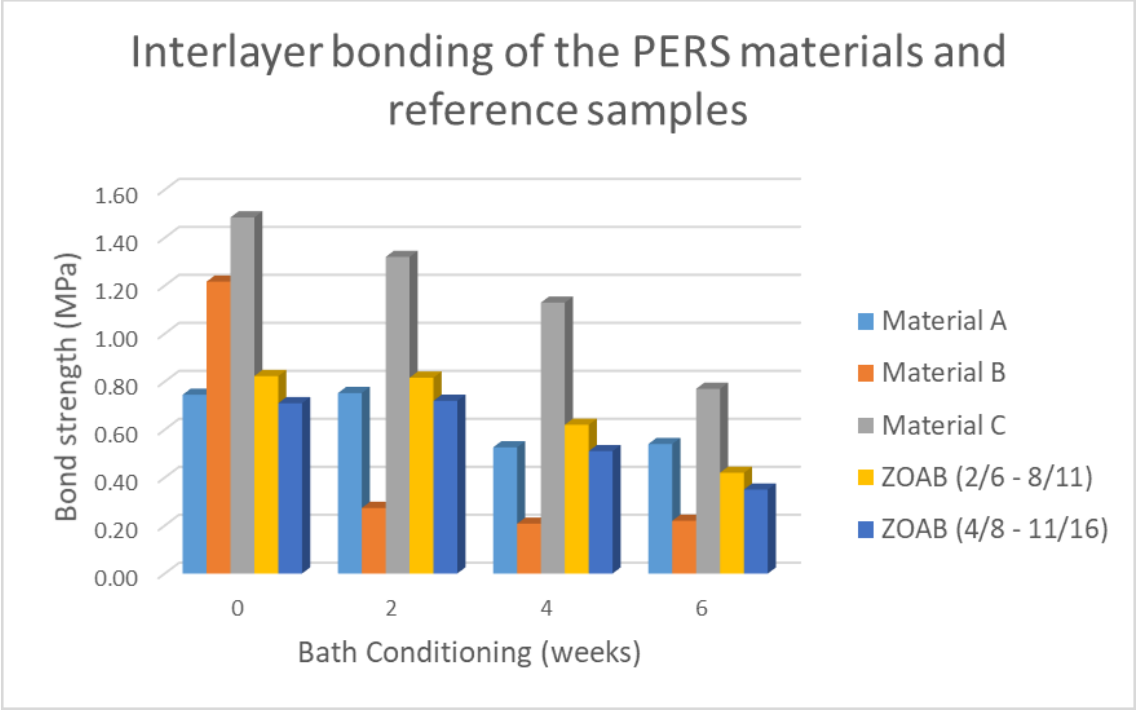

Graph 14. Variation of interlayer bonding over time of bath conditioning for LNRS and reference materials

Similarly, to the ITSR an adhesive strength ratio, which indicates the effects of moisture susceptibility in the bond strength, is calculated based on formula (9). The results are presented in Table 10.

Table 10. ASR ratios of the 3 samples and the 2 reference samples

ASR (%)	2 weeks	4 weeks	6 weeks
Material A	100.9	70.6	72.4
Material B	22.5	17.1	18.1
Material C	88.9	76.1	51.9
ZOAB(2/6 - 8/11)	99.2	75.3	51.0
ZOAB(4/8 - 11/16)	101.4	71.8	49.3

5.3.2. Discussion of the results

Most of the samples experienced adhesive failure as it can be seen in Figures 20 to 22. An exception was the samples of Material A and Material C after two weeks of moisture conditioning that failed at the ZOAB layer.

Figure 20. Material A

Figure 21. Material B

Figure 22. Material C

A comparison of the results of the bond strengths for the three (3) LNRS-ZOAB with the already applied two-layer ZOAB reference systems indicates that Material A is close to the behavior of the already applied systems. On the other hand, Material C showed higher bond strength, thus better behavior. Material B failed in a low application of force, which results in poor bonding of the two layers.

Furthermore, it is clear that with increasing time of bath conditioning the interlayer bond becomes poorer. This decrease of adhesion strength is dramatic for Material B, which shows that it does not manage to establish a proper interaction of the LNRS-ZOAB system at wet conditions. This may be the consequence of using a highly moisture susceptible polyurethane to bind the aggregates.

The reference samples can be used as a limit under which the three (3) materials can be characterized insufficient. An average minimum tensile bond strength for each bath condition is set as criterion. Material A lays in between the values of the two reference two-layer ZOAB systems for the various conditions, whereas Material C has higher values that indicate strong bond between the layers. Material B fails at all wet conditions, as its values are lower from the two reference systems. ASR ratios indicate once again this fact and result that Material B is not able to resist water degradation, regarding its bonding properties.

6. Conclusions

The main conclusions that are extracted from the execution of the stiffness test, the indirect tension test and the interlayer bonding test are summarized below for the three (3) materials.

- Material C is stiffer than Material A and B, whereas Material A is the most flexible. This is mainly affected by the mixture composition of Material C, which lacks totally of rubber, resulting to poor elasticity.
- Material A and Material B maintain their stiffness levels over the loading frequency range based on the sufficient content of rubber particles.
- On the other hand, the stiffness of Material C ranges between the values of the other two for low frequencies and becomes too stiff for high frequencies. This may lead to problems related to low-temperature cracking in the field.
- The indirect tensile strength of Material A is slightly affected by bath and MiST conditioning and behaves well enough in presence of water.
- Material B has low tensile strength after bath and MiST in time, and consequently low ITSR values, which translates to high water susceptibility of the material.
- The indirect strength values of Material C fluctuate at the various conditions but fulfil the ITSR Dutch specifications. Probably, the high percentage of polyurethane results in sufficient strength independently to moisture conditioning.
- All samples of Material B failed at the interface between the layers, whereas Material A and C failed in cohesion at the ZOAB layer after two (2) weeks of bath conditioning.
- Material B failed at the interface of the LNRS-ZOAB system in presence of water, probably due to the use of a highly moisture susceptible polyurethane glue.
- Material C appears to have the best bonding between the two layers, whereas the bond strength of Material B lies between the values of the two (2) reference ZOAB-ZOAB systems.
- Overall evaluation of the three shows that Material B does not satisfy the requirements for a LNRS material.
- The other two materials behave properly enough in these mechanical tests and further evaluation is required to take a more detailed overview of the different properties.

7. References

[1] L. Goubert, "Development of the ultra low noise poroelastic road surface: the findings of the persuade project," *Conference Proceedings of the 23rd International Conference on Sound and Vibration,Greece,* 2016.

[2] U. Sandberg and L. Goubert, "Poroelastic Road Surface (PERS): A review of 30 years of R&D work," *Conference Proceedings of the 40th international Congress and Exposition on Noise Control Engineering, INTER-NOISE, Osaka, Japan,* 2011.

[3] U. Sandberg, L. Goubert, K. P. Billigri and B. Kalman, "PERSUADE: Poroelastic road surface: an innovation to avoid damages to environmnet.State-of-the-Art regarding poroelastic road surfaces," 2010.

[4] A. J. Ejsmont, L. Goubert, B. Ronowski and G. Swieczko-Zurek, "Ultra low noise poroelastic road surfaces," 2016.

[5] U. Sandberg and L. Goubert, "PERSUADE - A European project for exceptional noise reduction by means of poroelastic road surfaces," *Inter-noise, Osaka,* 2011.

[6] L. Goubert, "Construction and Performance of Poroelastic Road Surfaces Offering 10 dB of Noise Reduction. Policy brief," *PoroElastic Road SUrface: an innovation to Avoid Damages to the Environment,* 2016.

[7] L. Goubert and U. Sandberg, "The PERSUADE project: developing the concept of poroelastic road surface into a powerful tool for abating traffing noise," *Inter-noise, Lisbon, Portugal,* 2010.

[8] H. D. Benedetto, M. N. Partl, L. Francken and C. De La Roche Saint André, "Stiffness testing for bituminous mixtures," *RILEM TC 182-PEB PERFORMANCE TESTING AND EVALUATION OF BITUMINOUS MATERIALS,* 2001.

[9] T. Pellinen, "Investigation of the use of dynamic modulus as an indicator of hot-mix asphalt performance," *PhD dissertation, Arizona State University, Tempe, Arizona,* 2001.

[10] K. P. A. Biligiri, B. Kalman and A. Samuelson, "Understanding the fundamental material properties of low-noise poroelastic road surfaces," *International Journal of Pavement engineering,* pp. 12-23, 2013.

[11] T. O. Medani and M. Huurman, "Constructing the Stiffness Master Curves for Asphaltic Mixes," *Report 7-01-127-3, Delft University of Technology, Netherlands,* 2003.

[12] L. Francken and C. Clauwaert, "Characterization and Structural Assesment of Bound Materials for Flexible Road Structures," 1988.

[13] R. Lytton, U. J., E. Fernando, R. Roque, D. Hiltunen and S. Stoffels, "Development and Validation of Performance Prediction Models and Specifications for Asphalt Binders and Paving Mixes," 1993.

[14] M. Jacobs, "Crack growth in Asphaltic Mixes," 1995.

[15] R. Hicks, "NCHRP Synthesis of Highway Practice 175: Moisture damage in asphalt concrete," *Washington D.C.,TRB and National Research Council,* 1991.

[16] N. Kringos and A. Scarpas, "Ravelling of asphaltic mixes due to water damage: Computational identification of controlling parameters," *Transportation Research Board: Journal of the Transportation Board,* pp. 79-87, 2005.

[17] P. Kandhal and I. Rickards, "Premature failure of asphalt overlays from stripping: Case histories," *National Center for Asphalt Technology of Auburn University, Alabama,* 2001.

[18] CEN, "European Committee for standardization Bituminous mixtures NEN-EN12697-12: bituminous mixtures - Test methods for hot mix asphalt- art 12: Determination of the water sensitivity of bituminous specimens," 2003.

[19] S. Caro, E. Masad, A. Bhasin and D. Little, "Moisture susceptibility of asphalt mixtures, part 1: Mechanisms.," 2008.

[20] I. Inc., "Moisture Induced Sensitivity Test Operators Guide,Raleigh NC," 2012.

[21] A. Varveri, S. Avgerinopoulos and A. Scarpas, "Experimental evaluation of long and short term moisture damage characteristics of asphalt mixtures. Road Materials and Pavement Design," 2015.

[22] CEN, "European Committee for standardization NEN-EN 12697-23 : Bituminous Mixtures-Test methods for hot mix asphalt- Part 23 : Determination of the indirect tensile strength of bituminous specimens," 2004.

[23] CEN, "European Committee for standartization, NEN-EN 12697-46: Bituminous Mixtures - Test Methods for hot mix asphalt- Part 46: Low temperature cracking and properties by unaxial tension tests," 2012.

[24] C. Raab and M. N. Parti, "Evaluation of interlayer shear bond devices for asphalt pavements," *The baltic Journal of Road and Bridge Enginnering,* 2009.

[25] R. Hofman, P. The and v. V. Wilemjan, "Results Dutch PERS test on A50.," *Conference proceedings of the 40th International Congress and Exposition on Noise Control Engineering, INTER-NOISE, Osaka, Japan,* 2011.

[26] R. Dongre, L. Myers, J. D'Angelo, C. Paugh and J. Gudimettla, "Field Evaluation of Witczak and Hirsch Models for Predicting Dynamic Modulus of Hot-Mix Asphalt (With Discussion)," *Journal of the Association of Asphalt Paving Technologists: From the Proceedings of the Technical Sessions,* pp. 6-10, 2005.

[27] M. J. G. S. Erkens, "Asphalt Concrete response (ACRe) - Determination, modeling and prediction.," *PhD dissertation, Delft University of Technology, Netherlands,* 2002.

[28] F. Pramesti, "Laboratory and field apshalt fatigue performance," *PhD dissertation, Delft University of Technology, Netherlands,* 2015.